# Concatenation of Space-Time Block Codes with Convolutional Codes

Saajed Ali

Thesis submitted to the Faculty of the
Virginia Polytechnic Institute and State University
in partial fulfillment of the requirements for the degree of

Masters of Science
in
Electrical Engineering

Dr. Brian D Woerner, Chair
Dr. William H Tranter
Dr. Pushkin Kachroo

Feb 6, 2004
Blacksburg Virginia

Keywords: space-time codes, Rayleigh fading, convolutional codes, transmit-diversity, receive-diversity.

# Concatenation of Space-Time Block Codes with Convolutional Codes

Saajed Ali

(ABSTRACT)

Multiple antennas help in combating the destructive effects of fading as well as improve the spectral efficiency of a communication system. Receive diversity techniques like maximal ratio receive combining have been popular means of introducing multiple antennas into communication systems. Space-time block codes present a way of introducing transmit diversity into the communication system with similar complexity and performance as maximal ratio receive combining. In this thesis we study the performance of space-time block codes in Rayleigh fading channel. In particular, the quasi-static assumption on the fading channel is removed to study how the space-time block coded system behaves in fast fading. In this context, the complexity versus performance trade-off for a space-time block coded receiver is studied.

As a means to improve the performance of space-time block coded systems concatenation by convolutional codes is introduced. The improvement in the diversity order by the introduction of convolutional codes into the space-time block coded system is discussed. A general analytic expression for the error performance of a space-time block coded system is derived. This expression is utilized to obtain general expressions for the error performance of convolutionally concatenated space-time block coded systems utilizing both hard and soft decision decoding. Simulation results are presented and are compared with the analytical results.

# Acknowledgements

I would like to thank my advisor Dr. Brian D. Woerner for suggesting the thesis topic and for providing guidance throughout this work. His advice and supervision gave direction to this research. By providing opportunity to work on a number of research projects he helped me develop my capabilities for research and independent thinking.

I would also like to thank Dr. William. H. Tranter for the invaluable advice he provided throughout this research. His "computer aided design of communication systems" class proved to be of great help in the completion of this work. My thanks also go to Dr. Pushkin Kachroo for his insight into my work. I appreciate the enthusiasm and encouragement he showed towards this research. Special thanks also go to staff and all the student researchers at MPRG for their help and support.

# Contents

# List of Figures

# List Of Tables

# Chapter 1

# Introduction

## 1.1 Introduction

This chapter gives a brief overview of the thesis and the motivation behind the research work. A brief historical prospective to space-time codes is also presented. At the end a short overview of the chapters in this work and their organization is provided.

## 1.2 Overview

The purpose of this research is to study performance of space-time block codes in fading channels. The diversity advantage by introducing space-time block codes in a communication system is studied. The quasi-static constraint on fading channels is removed and its effect on the performance of space-time block coded systems is addressed.

In order to further improve the performance of space-time block coded systems in fading channels, concatenation by convolutional codes is introduced. Performance bounds for hard and soft decision decoding are obtained. It is seen how the introduction of convolutional codes into the space-time block coded system increases the diversity order. Numerous simulations results are presented to support the theoretical results.

## 1.3 Motivation

Multiple antennas in a communication system serve two important purposes. First they introduce diversity into the communication system. Second they also increase the capacity of communication systems.

Multi-paths in a wireless channel can introduce severe attenuation into the transmitted signal. Diversity techniques provide effective ways to combat the destructive nature of fading channels. Multiple antennas in a communication system provide diversity by utilizing the different channel characteristics between each pair of transmit and receive antennas.

The capacity increase due to the use of multiple antennas is studied in [1] [2] [3]. It is shown in these papers that the capacity of a multiple antenna communication system far exceeds that of a single antenna system. Analysis in [1] shows that as long as the number of receive antennas is greater than or equal to the number of transmit antennas, the capacity of multiple antenna systems grows at least linearly with the number of transmit antennas.

Due to the above-mentioned benefits the use of multiple antennas in communication systems working under the constraints of severe fading is becoming increasingly popular. Cellular-service providers invariably use multiple antennas to combat fading. A common practice in cellular industry is to have two receive antennas per sector to introduce receive diversity into the communication system.

Space-time block codes present a means of introducing transmit diversity into the base station with performance results similar to the receive diversity techniques. With the introduction of space-time block coding the base station can provide reliable communication not only from the mobile user to the base station (receive diversity) but also from the base station to the mobile user (transmit diversity). We cannot typically use the receive diversity techniques for the mobile station because it has size constraints and it may not be practical to deploy more than a single antenna on it. Further more even if we use multiple antennas on the receiver, we may not get enough separation between the antennas for an effective diversity advantage. Space-time codes provide the communication system engineer effective means to bypass this difficulty.

Mobile wireless devices are increasingly becoming an essential entity in our daily lives. We use wireless phones at home, offices and while traveling on the road. Due to the widespread use of wireless devices in every possible scenario, it is important for wireless services to be robust. In this context it is essential for practical space-time codes to have acceptable performance in fast fading channels. In this thesis the quasi-static assumption on space-time block coded communication systems is removed to examine its behavior in fast fading channels. The complexity versus performance trade-off for a space-time block coded receiver is studied. It is seen how performance starts deteriorating with increasing Doppler for the quasi-static receiver. As a means to improve the performance of the space-time block coded system concatenation with convolutional codes is introduced. Convolutional codes improve the performance of space-time block coded systems by increasing their diversity. The concatenation scheme provides the systems engineer a method of improving the diversity without using additional antennas. This advantage however comes with the cost of additional complexity and introduction of interleaving delays.

## *1.4 Previous research and contribution of the thesis*

Transmit diversity techniques received extensive attention after the introduction of space-time codes. Some early transmit diversity schemes were introduced in [4], [5] and [6]. Tarokh et al. introduced space-time trellis coding as a transmit diversity technique in [7]. In this scheme joint designs for transmit diversity, channel coding and modulation were proposed. Space-time trellis codes were shown to have good performance at the cost of higher complexity. For a fixed number of transmit antennas the decoding complexity of space-time trellis codes was shown to grow exponentially as a function of bandwidth efficiency and the diversity level. Alamouti in [8] introduced a two transmit antenna scheme which utilized very simple transmit and receive processing while still retaining the full diversity order without any bandwidth expansion. Further work on this scheme was done by Tarokh et al. in [9] and [10]. The two-antenna scheme introduced by Alamouti was extended to more than two antennas. [9] introduced the general theory for space-time block code construction. It was shown that for real signals space-time block codes could be designed to give full diversity at the maximum possible transmission rate. For complex constellation signaling new codes were designed that provided full diversity at half and three-fourths of the maximum transmission rate. [10] provides simulation results for the error performance of the newly proposed space-time block codes at different bandwidth efficiencies. Recently, moderate complexity diagonal algebraic space-time block codes (DAST) have been designed which can provide full diversity while maintaining their transmission rate. These codes however are not as simple as Alamoutis space-time block codes.

In this work the performance of space-time block codes in Rayleigh fading is studied. It is shown that for a quasi-static channel the receiver maintains a simple structure and the receiver processing is reduced to symbol-by-symbol ML detection. Two scenarios are considered for fast fading channels. In the first case the receiver assumes the channel to be quasi-static, maintaining its simple structure. Simulation results are presented that show how performance degrades with increasing Doppler. In the second case the receiver no longer assumes the channel to be quasi-static so that it performs significant processing for signal detection. Simulation results are presented that show no performance deterioration in fast fading. The performance versus complexity trade-off is studied for fast fading channels.

It may not be possible to estimate all channel coefficients perfectly for a fast fading channel. Simulation results are presented that show the performance of space-time block coded systems when only some channel coefficients are estimated perfectly and the rest are the interpolated values of these.

In order to further improve the performance of the space-time block coded systems, serial concatenation with convolutional codes is studied. It is seen how convolutional codes further increase the diversity of the communication system. General expressions for the error performance of convolutionally concatenated space-time block coded systems are derived for both hard and soft decision decoding. It is shown that the diversity order increases to $N_T \times N_R \times dfree/2$ for hard decision decoding and $N_T \times N_R \times dfree$ for soft decision decoding, where $N_T$ is the number of transmit antennas, $N_R$ the number of receive antennas and $dfree$ is the free distance of the convolutional code. Simulation results are provided that verify the analytical results.

## *1.5 Organization of chapters*

Chapter 2 introduces space-time block codes and provides simulation results showing its BER performance in Rayleigh fading. The construction of space-time block codes is discussed and it is shown how orthogonality and the quasi-static assumption lead to simplified processing at the receiver. In order to evaluate the performance of space-time block codes without the quasi-static assumption, simulation results are provided at different Dopplers. Receiver complexity versus BER performance trade-off is also addressed in this chapter. This chapter also touches the real life scenario of having imperfect channel estimation and provides simulation results for such a case.

In Chapter 3 analytic bounds for the error performance of arbitrary orthogonal space-time block codes in Rayleigh fading channels are derived. A brief introduction to convolutional coding is given and expressions for the performance of convolutionally coded systems in Rayleigh fading are derived. This chapter introduces convolutionally concatenated space-time block coding schemes. General analytic expressions for the error performance of the concatenated scheme using hard and soft decision decoding are derived. Simulation results are provided to verify the analytical results.

Chapter 4 presents the conclusions of this work. The contributions of this work and the scope of future research are also discussed.

# Chapter 2

# Space-time block coding fundamentals

## *2.1 Introduction*

This chapter gives an introduction to space-time block codes. Since the receive combining for MRRC resembles that for space-time block codes, this chapter reviews MRRC techniques for receive diversity. Alamouti's simple two transmit antenna space-time block code is discussed, followed by the more generalized space-time block codes as introduced by Tarokh et al. Properties of orthogonal design are also discussed and it is shown how this leads to a simplified receiver structure.

This chapter also introduces the impact of time varying Rayleigh fading channel on the performance of space-time block coded systems. Simulations are performed under different scenarios. The performance of space-time block coded systems in a quasi-static channel; a time varying flat Rayleigh fading channel with and without a quasi-static receiver is studied. A simple linear interpolation technique is introduced which serves as a compromise between the case of the quasi-static receiver and the case where the receiver has perfect knowledge of all the channel coefficients within each code frame.

## *2.2 Diversity*

Multi-path fading in a wireless channel can cause severe degradation in the performance of a communication system. In order to mitigate the effects of fading, diversity techniques are used. These techniques are commonly classified into the following categories:

**Spatial diversity**: If transmission and reception of information is carried out via multiple antennas placed at appropriate distances in space and suitable processing done, performance in fading channels can be improved. The three most common space diversity techniques employed at the receiver are selection combining, maximal ratio combining and equal gain combining. In selection combining (SC) multiple receive antennas are placed at large enough distances so that fading is independent in each receive antenna. The best signal from all the receive antennas is selected for detection. In maximal ratio combining (MRC) the channel is estimated and the signals received by each receive antenna are weighed according to the estimates so as to maximize the SNR. In equal gain combining (EGC) weights are not dependent on the channel estimates. Signals from each receive antenna are multiplied by the same weight so as to give a lower SNR performance when compared to MRC. Even though the performance for EGC is lower than for MRC, no channel estimation needs to be done in EGC.

**Polarization diversity**: Orthogonally polarized waves with independent fading characteristics can be used as a source of diversity. Such techniques are called polarization diversity techniques. In urban environments where space is limited, polarization diversity is particularly advantageous as we can place antennas together. It however provides only two diversity branches. In environments with a number of reflections, the polarization may ultimately be lost and this technique may no longer be useful. Line of sight communications can use polarization diversity to better its performance.

**Frequency diversity**: If data is sent on carriers sufficiently spaced apart in frequency, fading can be considered to be independent. We define coherence bandwidth of a channel as [11]

*Coherence bandwidth is the range of frequencies over which two frequency components have strong amplitude correlation.*

Based on this definition we can have different measures of coherence bandwidth depending on how high a value of correlation we may want to use.

Thus we may say that if data is sent on carriers that are spaced by more than the coherence bandwidth of the channel we can utilize frequency diversity.

**Time diversity:** If the transmitted signal is repeated in time and the interval of time between repetitions is large enough for the channel characteristics to change, the received signals can undergo independent fading. We define coherence time of the channel as [11]

*Coherence time is the statistical measure of time during which the two received signals have strong amplitude correlation.*

Based on this definition we can have different measures of coherence time depending on how high a value of correlation we may want to use.

Thus we may say that if data is repeated in time with time duration greater than the coherence time of the channel we can utilize time diversity. If the data rate is fixed, higher Doppler will provide greater time diversity though not necessarily better signal as higher Doppler means deeper fades.

## 2.3 Maximal ratio receive combining

Consider a single transmitter and $n$ receivers. Let the transmitted symbol be $\boldsymbol{c} \in \boldsymbol{S}$, where $\boldsymbol{S}$ is the finite set of possible symbols that can be transmitted. Assuming the channel to be flat, let the path gains from the transmit antenna to the $j$th receive antenna be $\boldsymbol{\alpha}_j, j = 1,2,3 \ldots n$. Let the average energy of each symbol transmitted be normalized to unity. Let $\boldsymbol{n}_j, j = 1,2,3 \ldots n$ represent zero mean complex Gaussian noise with variance $\sigma_x = \sigma_y$ per complex dimension. If $SNR$ is the signal to noise ratio, then

$$SNR = \frac{1}{2\sigma_x^2} = \frac{1}{2\sigma_y^2}$$

or variance per complex dimension is $1/(2SNR)$.

Let $\boldsymbol{r}_j, j = 1, 2 \ldots n$ are the received signals, then

$$\boldsymbol{r}_j = \boldsymbol{\alpha}_j \boldsymbol{c} + \boldsymbol{n}_j \qquad j = 1, 2,3 \ldots n \tag{2.1.1}$$

If the channel is perfectly estimated, the receiver decision metric is

$$\sum_{j=1}^{n} \left| \boldsymbol{r}_j - \boldsymbol{\alpha}_j \boldsymbol{s} \right|^2 \tag{2.1.2}$$

The symbol $\boldsymbol{s} \in \boldsymbol{S}$ that minimizes the sum is chosen.

For two-antenna case, the above metric reduces to:

$$-(\boldsymbol{\alpha}_1^* \boldsymbol{r}_1 + \boldsymbol{\alpha}_2^* \boldsymbol{r}_2)\boldsymbol{s}^* - (\boldsymbol{\alpha}_1 \boldsymbol{r}_1^* + \boldsymbol{\alpha}_2 \boldsymbol{r}_2^*)\boldsymbol{s} + (|\,\boldsymbol{\alpha}_1\,|^2 + |\,\boldsymbol{\alpha}_2\,|^2)\,|\,\boldsymbol{s}\,|^2 \tag{2.1.3}$$

Let

$$\hat{\boldsymbol{s}} = (\boldsymbol{\alpha}_1^* \boldsymbol{r}_1 + \boldsymbol{\alpha}_2^* \boldsymbol{r}_2) \tag{2.1.4}$$

Minimizing (2.1.3) is the same as minimizing

$$|\hat{\boldsymbol{s}} - \boldsymbol{s}|^2 + (|\boldsymbol{\alpha}_1|^2 + |\boldsymbol{\alpha}_2|^2)|\boldsymbol{s}|^2 \qquad \forall \boldsymbol{s} \in \boldsymbol{S} \tag{2.1.5}$$

For equal energy signals (2.1.5) reduces to

$$|\hat{\boldsymbol{s}} - \boldsymbol{s}|^2 \qquad \forall \boldsymbol{s} \in \boldsymbol{S} \tag{2.1.6}$$

The ML detector can be used to estimate $\boldsymbol{c}$ by choosing $\boldsymbol{s}$ with minimum Euclidian distance.

Using (2.1.4) and (2.1.1)

$$\hat{\boldsymbol{s}} = (|\boldsymbol{\alpha}_1|^2 + |\boldsymbol{\alpha}_2|^2)\boldsymbol{c} + \boldsymbol{\alpha}_1^* \boldsymbol{n}_1 + \boldsymbol{\alpha}_2^* \boldsymbol{n}_2$$

it is seen how diversity helps in improving performance. If the channels between the transmit antenna and the two receive antennas are assumed to be uncorrelated there is a good likelihood of having a strong signal in one of the channels even if the other is in a deep fade.

Fig 2.1 shows the performance of MRRC in Rayleigh fading. BPSK modulation is used. Fading is assumed to be uncorrelated. Perfect knowledge of the channel is also assumed. The energy of symbols transmitted is normalized to unity.

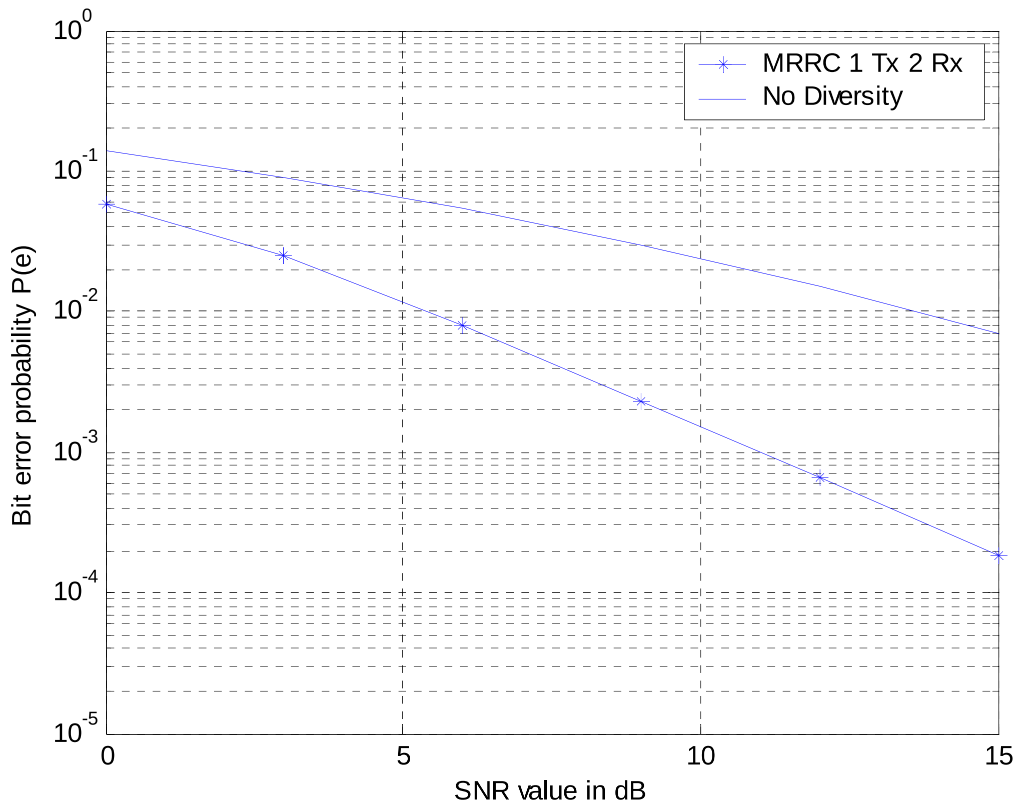


**Fig 2. 1:** BER performance comparison of systems without diversity and with MRRC (1 Tx, 2 Rx) in Rayleigh fading and BPSK modulation.

## *2.4 Space-time block coding*

### *2.4.1 Alamouti scheme*

Alamouti [8] showed that performance improvement similar to MRRC can be achieved using a simple new transmit diversity scheme. The scheme is particularly useful because it is easier and more economical to have multiple antennas at base stations rather than at remote units. A description of the proposed scheme is given below.

Consider a two transmit and one receive antenna communication system. At time $t$, $t = 1,2$ signal $\boldsymbol{c}_t^i$, $i = 1,2$ is transmitted from the $i$th transmit antenna. Assuming the channel to be flat, let the path gains from the transmit antenna $i$ to the receive antenna be $\alpha_i$. Alamouti's space-time code is given as [8]

$$\begin{pmatrix} \boldsymbol{x}_1 & \boldsymbol{x}_2 \\ -\boldsymbol{x}_2^* & \boldsymbol{x}_1^* \end{pmatrix}$$

$\boldsymbol{x}$'s and their conjugates are variables that constitute the code matrix. Symbols are grouped in pairs and replace $\boldsymbol{x}$'s in the code matrix. The first row represents signals transmitted at time $t = 1$ and the second row represents the signals transmitted at time $t = 2$. The first column represents signals transmitted from antennal 1 and the second column represents signals transmitted from antenna 2.

The channel is assumed to be Rayleigh distributed and quasi-static, i.e. the channel coefficients do not change during the transmission of the code block. Let the average energy of each symbol transmitted be normalized to unity. Let $\boldsymbol{n}_t, t = 1,2$ represent zero mean complex Gaussian noise with variance $2/(2SNR)$ per complex dimension, where *SNR* is the signal to noise ratio. A factor of 2 in the numerator appears because we are considering two transmit antennas. Let $\boldsymbol{S}$ be the finite set of all possible symbols that can be transmitted. If $\boldsymbol{r}_t, t = 1,2$ are the received signals and $\widetilde{\boldsymbol{s}}_i \in \boldsymbol{S}, i = 1,2$ are symbols input to the space-time block encoder then

$$\boldsymbol{r}_1 = \boldsymbol{\alpha}_1 \widetilde{\boldsymbol{s}}_1 + \boldsymbol{\alpha}_2 \widetilde{\boldsymbol{s}}_2 + \boldsymbol{n}_1 \tag{2.1.7}$$

$$\boldsymbol{r}_2 = -\boldsymbol{\alpha}_1 \widetilde{\boldsymbol{s}}_2^* + \boldsymbol{\alpha}_2 \widetilde{\boldsymbol{s}}_1^* + \boldsymbol{n}_2 \tag{2.1.8}$$

If the channel is perfectly estimated the receiver decision metric is

$$\sum_{t=1}^{2} \left| \boldsymbol{r}_t - \sum_{i=1}^{2} \boldsymbol{\alpha}_i \boldsymbol{c}_t^i \right|^2 \tag{2.1.9}$$

The symbol pair $(\boldsymbol{s}_1, \boldsymbol{s}_2) \in \boldsymbol{S}$ that minimizes the sum is chosen.

After evaluating the summation (2.1.9) we see that all the cross $\boldsymbol{s}$ terms cancel out and our task reduces to the independent minimization of

$$\left| \boldsymbol{\alpha}_1^* \boldsymbol{r}_1 + \boldsymbol{\alpha}_2 \boldsymbol{r}_2^* - \boldsymbol{s}_1 \right|^2 + \left( -1 + |\boldsymbol{\alpha}_1|^2 + |\boldsymbol{\alpha}_2|^2 \right) |\boldsymbol{s}_1|^2 \tag{2.1.10}$$

$$\left| \boldsymbol{\alpha}_2^* \boldsymbol{r}_1 + \boldsymbol{\alpha}_1 \boldsymbol{r}_2^* - \boldsymbol{s}_2 \right|^2 + \left( -1 + |\boldsymbol{\alpha}_1|^2 + |\boldsymbol{\alpha}_2|^2 \right) |\boldsymbol{s}_2|^2 \tag{2.1.11}$$

Let

$$\hat{\boldsymbol{s}}_1 = (\boldsymbol{\alpha}_1^* \boldsymbol{r}_1 + \boldsymbol{\alpha}_2 \boldsymbol{r}_2^*) \tag{2.1.12}$$

$$\hat{\boldsymbol{s}}_2 = (\boldsymbol{\alpha}_2^* \boldsymbol{r}_1 - \boldsymbol{\alpha}_1 \boldsymbol{r}_2^*) \tag{2.1.13}$$

Minimizing (2.1.10) and (2.1.11) is the same as minimizing

$$\left|\hat{\boldsymbol{s}}_1-\boldsymbol{s}_1\right|^2+\left(-1+|\boldsymbol{\alpha}_1|^2+|\boldsymbol{\alpha}_2|^2\right)|\boldsymbol{s}_1|^2 \tag{2.1.14}$$

$$\left|\hat{\boldsymbol{s}}_2-\boldsymbol{s}_2\right|^2+\left(-1+|\boldsymbol{\alpha}_1|^2+|\boldsymbol{\alpha}_2|^2\right)|\boldsymbol{s}_2|^2 \tag{2.1.15}$$

For equal energy signals (2.1.14) and (2.1.15) reduce to

$$\left|\hat{\boldsymbol{s}}_1-\boldsymbol{s}_1\right|^2$$

$$\left|\hat{\boldsymbol{s}}_2-\boldsymbol{s}_2\right|^2$$

$\forall \boldsymbol{s} \in \boldsymbol{S}$ .

The ML detector can be used to estimate $\widetilde{\boldsymbol{s}}$ by choosing $\boldsymbol{s}$ with minimum Euclidian distance.

Using (2.1.7), (2.1.8), (2.2.12) and (2.1.13)

$$\hat{\boldsymbol{s}}_1=(|\boldsymbol{\alpha}_1|^2+|\boldsymbol{\alpha}_2|^2)\widetilde{\boldsymbol{s}}_1+\boldsymbol{\alpha}_1^*\boldsymbol{n}_1+\boldsymbol{\alpha}_2\boldsymbol{n}_2^*$$

$$\hat{\boldsymbol{s}}_2=(|\boldsymbol{\alpha}_1|^2+|\boldsymbol{\alpha}_2|^2)\widetilde{\boldsymbol{s}}_2+\boldsymbol{\alpha}_1\boldsymbol{n}_2^*+\boldsymbol{\alpha}_2^*\boldsymbol{n}_1$$

it is seen how diversity helps in improving performance. If the channels between the two transmit antennas and the receive antenna are assumed to be uncorrelated there is a good likelihood of having a strong signal from one of the channels even if the other is in a deep fade.

Fig 2.2 shows the performance of Alamouti's space-time code in Rayleigh fading. BPSK modulation is used. Fading is assumed to be uncorrelated. Perfect knowledge of the channel is also assumed. The energy of symbols from each transmit antenna is assumed to be 1.

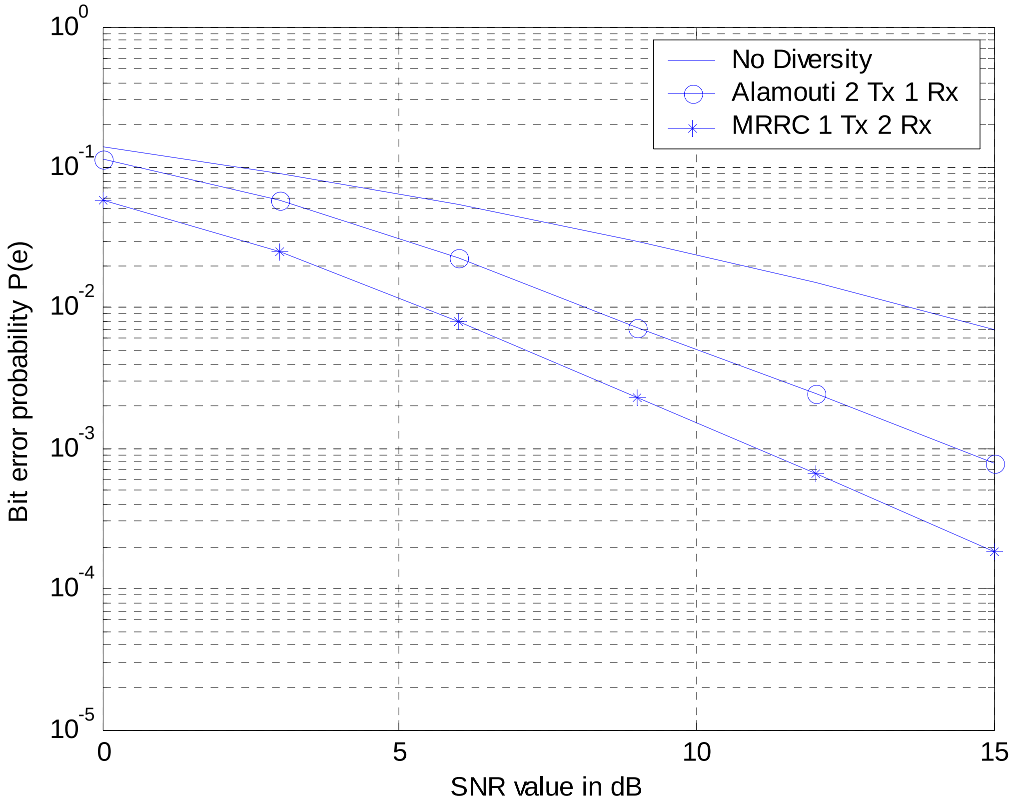


**Fig 2. 2:** BER performance comparison of systems without diversity, MRRC (1 Tx, 2 Rx), STBC (2 Tx, 1 Rx) in Rayleigh fading with BPSK modulation.

The simulation for the Alamouti scheme assumes that each transmit antenna transmits at unit power. The total transmitted power is twice that in MRRC. Therefore there is a 3 dB loss for the Alamouti scheme when compared to MRRC.

### *2.4.2 Generalized orthogonal space-time block codes*

Alamouti's two transmit antenna scheme is remarkable because of its simplicity. After the scheme was proposed there has been wide spread research into the design of simple new codes that would utilize multiple transmit antennas. Tarokh et al. [9] used the theory of orthogonal designs to come up with more space-time block codes for multiple transmit antennas.

We first generalize our wireless communication system to $N_T$ transmit antennas and $N_R$ receive antennas. At time *t,* signals $\boldsymbol{c}_t^i$, $i = 1,2 \ldots N_T$ are transmitted simultaneously from the $N_T$ transmit antennas. These signals are linear combinations of

$k$ symbols $(\boldsymbol{s}_1, \boldsymbol{s}_2 \ldots \boldsymbol{s}_k) \in \boldsymbol{S}$, and their conjugates. $\boldsymbol{S}$ is the finite set of possible symbols that can be transmitted. Assuming the channel to be flat, let the path gains from the transmit antenna *i* to the receive antenna *j* be $\alpha_{i.j}$. The encoding scheme maps *k*-input symbols to $N_T$ sequences of length *p*. This gives a code rate *r* of $k/p$. The wireless channel is assumed to be quasi-static so that the path gains are constant through the transmission of the entire frame of length *p*. The received signal at antenna *j* and at time *t* is given by

$$\boldsymbol{r}_t^j = \sum_{i=1}^{N_T} \boldsymbol{\alpha}_{i,j} \boldsymbol{c}_t^i + \boldsymbol{n}_t^j$$

where $\boldsymbol{n}_t^j$ represent zero mean complex Gaussian noise with variance $N_T/(2SNR)$ per complex dimension, where *SNR* is the signal to noise ratio. The average energy of the symbols transmitted from each antenna is normalized to one so that average energy received at each receive antenna is $N_T$.

Assuming perfect CSI, the receiver evaluates the following decision metric

$$\sum_{t=1}^{p} \sum_{j=1}^{N_R} \left| \boldsymbol{r}_t^j - \sum_{i=1}^{N_T} \boldsymbol{\alpha}_{i,j} \boldsymbol{c}_t^i \right|^2 \tag{2.1.16}$$

Combinations of symbols taken from the symbol set $(\boldsymbol{s}_1, \boldsymbol{s}_2 \ldots \boldsymbol{s}_k)$ that minimize the metric are chosen.

Block codes need to be designed that

1. Simplify the receiver
2. Lead to maximum diversity order of $N_T \times N_R$.

Alamouti gave the first orthogonal space-time block code [8]

$$G_1 = \begin{pmatrix} \boldsymbol{x}_1 & \boldsymbol{x}_2 \\ -\boldsymbol{x}_2^* & \boldsymbol{x}_1^* \end{pmatrix} \qquad k = 2, N_T = 2, p = 2, r = 1$$

Tarokh et al. generalized Alamouti's scheme to more than two transmit antennas and constructed the following space-time block codes using orthogonal design techniques [9]

$$G_3 = \begin{pmatrix} \boldsymbol{x}_1 & \boldsymbol{x}_2 & \boldsymbol{x}_3 \\ -\boldsymbol{x}_2 & \boldsymbol{x}_1 & -\boldsymbol{x}_4 \\ -\boldsymbol{x}_3 & \boldsymbol{x}_4 & \boldsymbol{x}_1 \\ -\boldsymbol{x}_4 & -\boldsymbol{x}_3 & \boldsymbol{x}_2 \\ \boldsymbol{x}_1^* & \boldsymbol{x}_2^* & \boldsymbol{x}_3^* \\ -\boldsymbol{x}_2^* & \boldsymbol{x}_1^* & -\boldsymbol{x}_4^* \\ -\boldsymbol{x}_3^* & \boldsymbol{x}_4^* & \boldsymbol{x}_1^* \\ -\boldsymbol{x}_4^* & -\boldsymbol{x}_3^* & \boldsymbol{x}_2^* \end{pmatrix} \qquad k = 4, N_T = 3, p = 8, r = 1/2$$

$$G_3^{'} = \begin{pmatrix} \boldsymbol{x}_1 & \boldsymbol{x}_2 & \frac{\boldsymbol{x}_3}{\sqrt{2}} \\ -\boldsymbol{x}_2^* & \boldsymbol{x}_1^* & \frac{\boldsymbol{x}_3}{\sqrt{2}} \\ \frac{\boldsymbol{x}_3^*}{\sqrt{2}} & \frac{\boldsymbol{x}_3^*}{\sqrt{2}} & \frac{-\boldsymbol{x}_1 - \boldsymbol{x}_1^* + \boldsymbol{x}_2 - \boldsymbol{x}_2^*}{2} \\ \frac{\boldsymbol{x}_3^*}{\sqrt{2}} & -\frac{\boldsymbol{x}_3^*}{\sqrt{2}} & \frac{\boldsymbol{x}_2 + \boldsymbol{x}_2^* + \boldsymbol{x}_1 - \boldsymbol{x}_1^*}{2} \end{pmatrix} \qquad k = 3, N_T = 3, p = 4, r = 3/4$$

$$G_4 = \begin{pmatrix} \boldsymbol{x}_1 & \boldsymbol{x}_2 & \boldsymbol{x}_3 & \boldsymbol{x}_4 \\ -\boldsymbol{x}_2 & \boldsymbol{x}_1 & -\boldsymbol{x}_4 & \boldsymbol{x}_3 \\ -\boldsymbol{x}_3 & \boldsymbol{x}_4 & \boldsymbol{x}_1 & -\boldsymbol{x}_2 \\ -\boldsymbol{x}_4 & -\boldsymbol{x}_3 & \boldsymbol{x}_2 & \boldsymbol{x}_1 \\ \boldsymbol{x}_1^* & \boldsymbol{x}_2^* & \boldsymbol{x}_3^* & \boldsymbol{x}_4^* \\ -\boldsymbol{x}_2^* & \boldsymbol{x}_1^* & -\boldsymbol{x}_4^* & \boldsymbol{x}_3^* \\ -\boldsymbol{x}_3^* & \boldsymbol{x}_4^* & \boldsymbol{x}_1^* & -\boldsymbol{x}_2^* \\ -\boldsymbol{x}_4^* & -\boldsymbol{x}_3^* & \boldsymbol{x}_2^* & \boldsymbol{x}_1^* \end{pmatrix} \qquad k = 4, N_T = 4, p = 8, r = 1/2$$

$$G_4^{'} = \begin{pmatrix} \boldsymbol{x}_1 & \boldsymbol{x}_2 & \frac{\boldsymbol{x}_3}{\sqrt{2}} & \frac{\boldsymbol{x}_3}{\sqrt{2}} \\ -\boldsymbol{x}_2^* & \boldsymbol{x}_1^* & \frac{\boldsymbol{x}_3}{\sqrt{2}} & -\frac{\boldsymbol{x}_3}{\sqrt{2}} \\ \frac{\boldsymbol{x}_3^*}{\sqrt{2}} & \frac{\boldsymbol{x}_3^*}{\sqrt{2}} & \frac{(-\boldsymbol{x}_1 - \boldsymbol{x}_1^* + \boldsymbol{x}_2 - \boldsymbol{x}_2^*)}{2} & \frac{(-\boldsymbol{x}_2 - \boldsymbol{x}_2^* + \boldsymbol{x}_1 - \boldsymbol{x}_1^*)}{2} \\ \frac{\boldsymbol{x}_3^*}{\sqrt{2}} & -\frac{\boldsymbol{x}_3^*}{\sqrt{2}} & \frac{(\boldsymbol{x}_2 + \boldsymbol{x}_2^* + \boldsymbol{x}_1 - \boldsymbol{x}_1^*)}{2} & -\frac{(\boldsymbol{x}_1 + \boldsymbol{x}_1^* + \boldsymbol{x}_2 - \boldsymbol{x}_2^*)}{2} \end{pmatrix}$$

$$k = 3, N_T = 4, p = 4, r = 3/4$$

$\boldsymbol{x}$ and its conjugate represent variables whose linear combination constitute the code matrix. Symbols are grouped in sets of $k$ and each symbol in the set replaces $\boldsymbol{x}$'s in the code matrix. The *i*th row represents signals transmitted at time $t = i$. The *jth* column represents signals transmitted from antenna *j.*

If *G* represents any of the above code matrices, it can be shown that [9]

$$\boldsymbol{G}^*\boldsymbol{G} = \boldsymbol{D}$$

where *D* is a diagonal matrix whose diagonal elements are of the form

$$a_1 \mid \boldsymbol{x_1} \mid^2 + a_2 \mid \boldsymbol{x_2} \mid^2 + \ldots\ldots + a_k \mid \boldsymbol{x_k} \mid^2$$

$a_1, a_2, \ldots\ldots, a_k$ being positive.

The generalized orthogonality of the code matrix greatly simplifies the decision metric calculation for the quasi-static case. Orthogonality results in the decoupling of the decision metric into *k* separate metrics for the *k* symbols transmitted. Each metric then needs to be minimized separately, saving a lot of computational burden for the receiver. For example (2.1.10) and (2.1.11) give two independent metrics for the Alamouti's two transmitter one receiver case.

To illustrate this point further, consider the code $G_3$. If $(\boldsymbol{s_1}, \boldsymbol{s_2}, \boldsymbol{s_3}, \boldsymbol{s_4})$ are variables representing symbols belonging to $\boldsymbol{S}$, minimization of (2.2.16) reduces to the independent minimization of

$$\left|\left[\sum_{j=1}^{m}\left(\boldsymbol{r}_1^j\boldsymbol{\alpha}_{1,j}^* + \boldsymbol{r}_2^j\boldsymbol{\alpha}_{2,j}^* + \boldsymbol{r}_3^j\boldsymbol{\alpha}_{3,j}^* + (\boldsymbol{r}_5^j)^*\boldsymbol{\alpha}_{1,j} + (\boldsymbol{r}_6^j)^*\boldsymbol{\alpha}_{2,j} + (\boldsymbol{r}_7^j)^*\boldsymbol{\alpha}_{3,j}\right)\right] - \boldsymbol{s}_1\right|^2$$
$$+\left(-1 + 2\sum_{j=1}^{m}\sum_{i=1}^{3}\left|\boldsymbol{\alpha}_{i,j}\right|^2\right)\left|\boldsymbol{s}_1\right|^2 \qquad (2.1.17)$$

$$\left|\left[\sum_{j=1}^{m}\left(\boldsymbol{r}_1^j\boldsymbol{\alpha}_{2,j}^* - \boldsymbol{r}_2^j\boldsymbol{\alpha}_{1,j}^* + \boldsymbol{r}_4^j\boldsymbol{\alpha}_{3,j}^* + (\boldsymbol{r}_5^j)^*\boldsymbol{\alpha}_{2,j} + (\boldsymbol{r}_6^j)^*\boldsymbol{\alpha}_{1,j} + (\boldsymbol{r}_8^j)^*\boldsymbol{\alpha}_{3,j}\right)\right] - \boldsymbol{s}_2\right|^2$$
$$+\left(-1 + 2\sum_{j=1}^{m}\sum_{i=1}^{3}\left|\boldsymbol{\alpha}_{i,j}\right|^2\right)\left|\boldsymbol{s}_2\right|^2 \qquad (2.1.18)$$

$$\left|\left[\sum_{j=1}^{m}\left(\boldsymbol{r}_1^j\boldsymbol{\alpha}_{3,j}^* - \boldsymbol{r}_3^j\boldsymbol{\alpha}_{1,j}^* - \boldsymbol{r}_4^j\boldsymbol{\alpha}_{2,j}^* + (\boldsymbol{r}_5^j)^*\boldsymbol{\alpha}_{3,j} - (\boldsymbol{r}_7^j)^*\boldsymbol{\alpha}_{1,j} - (\boldsymbol{r}_8^j)^*\boldsymbol{\alpha}_{2,j}\right)\right] - \boldsymbol{s}_3\right|^2$$

$$+\left(-1+2\sum_{j=1}^{m}\sum_{i=1}^{3}\left|\boldsymbol{\alpha}_{1,j}\right|^2\right)\left|\boldsymbol{s}_3\right|^2 \quad (2.1.19)$$

$$\left|\left[\sum_{j=1}^{m}\left(-\boldsymbol{r}_2^j\boldsymbol{\alpha}_{3,j}^* + \boldsymbol{r}_3^j\boldsymbol{\alpha}_{2,j}^* - \boldsymbol{r}_4^j\boldsymbol{\alpha}_{1,j}^* - (\boldsymbol{r}_6^j)^*\boldsymbol{\alpha}_{3,j} + (\boldsymbol{r}_7^j)^*\boldsymbol{\alpha}_{2,j} - (\boldsymbol{r}_8^j)^*\boldsymbol{\alpha}_{1,j}\right)\right] - \boldsymbol{s}_4\right|^2$$

$$+\left(-1+2\sum_{j=1}^{m}\sum_{i=1}^{3}\left|\boldsymbol{\alpha}_{1,j}\right|^2\right)\left|\boldsymbol{s}_4\right|^2 \quad (2.1.20)$$

The symbols are decoupled because the quasi-static assumption assures that the cross $\boldsymbol{s}$ terms cancel out for the orthogonal code.

Let

$$\hat{\boldsymbol{s}}_1 = \sum_{j=1}^{m}\left(\boldsymbol{r}_1^j\boldsymbol{\alpha}_{1,j}^* + \boldsymbol{r}_2^j\boldsymbol{\alpha}_{2,j}^* + \boldsymbol{r}_3^j\boldsymbol{\alpha}_{3,j}^* + (\boldsymbol{r}_5^j)^*\boldsymbol{\alpha}_{1,j} + (\boldsymbol{r}_6^j)^*\boldsymbol{\alpha}_{2,j} + (\boldsymbol{r}_7^j)^*\boldsymbol{\alpha}_{3,j}\right) \quad (2.1.21)$$

$$\hat{\boldsymbol{s}}_2 = \sum_{j=1}^{m}\left(\boldsymbol{r}_1^j\boldsymbol{\alpha}_{2,j}^* - \boldsymbol{r}_2^j\boldsymbol{\alpha}_{1,j}^* + \boldsymbol{r}_4^j\boldsymbol{\alpha}_{3,j}^* + (\boldsymbol{r}_5^j)^*\boldsymbol{\alpha}_{2,j} + (\boldsymbol{r}_6^j)^*\boldsymbol{\alpha}_{1,j} + (\boldsymbol{r}_8^j)^*\boldsymbol{\alpha}_{3,j}\right) \quad (2.1.22)$$

$$\hat{\boldsymbol{s}}_3 = \sum_{j=1}^{m}\left(\boldsymbol{r}_1^j\boldsymbol{\alpha}_{3,j}^* - \boldsymbol{r}_3^j\boldsymbol{\alpha}_{1,j}^* - \boldsymbol{r}_4^j\boldsymbol{\alpha}_{2,j}^* + (\boldsymbol{r}_5^j)^*\boldsymbol{\alpha}_{3,j} - (\boldsymbol{r}_7^j)^*\boldsymbol{\alpha}_{1,j} - (\boldsymbol{r}_8^j)^*\boldsymbol{\alpha}_{2,j}\right) \quad (2.1.23)$$

$$\hat{\boldsymbol{s}}_4 = \sum_{j=1}^{m}\left(-\boldsymbol{r}_2^j\boldsymbol{\alpha}_{3,j}^* + \boldsymbol{r}_3^j\boldsymbol{\alpha}_{2,j}^* - \boldsymbol{r}_4^j\boldsymbol{\alpha}_{1,j}^* - (\boldsymbol{r}_6^j)^*\boldsymbol{\alpha}_{3,j} + (\boldsymbol{r}_7^j)^*\boldsymbol{\alpha}_{2,j} - (\boldsymbol{r}_8^j)^*\boldsymbol{\alpha}_{1,j}\right) \quad (2.1.24)$$

Minimising (2.1.17) through (2.1.20) is equivalent to minimizing

$$\left|\hat{\boldsymbol{s}}_1 - \boldsymbol{s}_1\right|^2 + \left(-1+2\sum_{j=1}^{m}\sum_{i=1}^{3}\left|\boldsymbol{\alpha}_{i,j}\right|^2\right)\left|\boldsymbol{s}_1\right|^2$$

$$\left|\hat{\boldsymbol{s}}_2 - \boldsymbol{s}_2\right|^2 + \left(-1+2\sum_{j=1}^{m}\sum_{i=1}^{3}\left|\boldsymbol{\alpha}_{i,j}\right|^2\right)\left|\boldsymbol{s}_2\right|^2$$

$$\left|\hat{\boldsymbol{s}}_3 - \boldsymbol{s}_3\right|^2 + \left(-1+2\sum_{j=1}^{m}\sum_{i=1}^{3}\left|\boldsymbol{\alpha}_{i,j}\right|^2\right)\left|\boldsymbol{s}_3\right|^2$$

$$\left|\hat{\boldsymbol{s}}_4 - \boldsymbol{s}_4\right|^2 + \left(-1+2\sum_{j=1}^{m}\sum_{i=1}^{3}\left|\boldsymbol{\alpha}_{i,j}\right|^2\right)\left|\boldsymbol{s}_4\right|^2$$

For equal energy signals these reduce to

$$\left|\hat{\boldsymbol{s}}_1 - \boldsymbol{s}_1\right|^2$$

$$\left|\hat{\boldsymbol{s}}_2 - \boldsymbol{s}_2\right|^2$$

$$\left|\hat{\boldsymbol{s}}_3 - \boldsymbol{s}_3\right|^2$$

$$\left|\hat{\boldsymbol{s}}_4 - \boldsymbol{s}_4\right|^2$$

$\forall \boldsymbol{s} \in \boldsymbol{S}$ .

The ML detector can be used to estimate $\widetilde{\boldsymbol{s}}$ by choosing $\boldsymbol{s}$ with minimum Euclidian distance.

Let $\widetilde{\boldsymbol{s}}_i \in \boldsymbol{S}, i = 1,2,3,4$ are symbols input to the space-time block encoder given by $G_3$ then the received signals are given by

$$\boldsymbol{r}_1^j = \boldsymbol{\alpha}_{1,j}\widetilde{\boldsymbol{s}}_1 + \boldsymbol{\alpha}_{2,j}\widetilde{\boldsymbol{s}}_2 + \boldsymbol{\alpha}_{3,j}\widetilde{\boldsymbol{s}}_3 + \boldsymbol{n}_1^j \tag{2.1.25}$$

$$\boldsymbol{r}_2^j = -\boldsymbol{\alpha}_{1,j}\widetilde{\boldsymbol{s}}_2 + \boldsymbol{\alpha}_{2,j}\widetilde{\boldsymbol{s}}_1 - \boldsymbol{\alpha}_{3,j}\widetilde{\boldsymbol{s}}_4 + \boldsymbol{n}_2^j \tag{2.1.26}$$

$$\boldsymbol{r}_3^j = -\boldsymbol{\alpha}_{1,j}\widetilde{\boldsymbol{s}}_3 + \boldsymbol{\alpha}_{2,j}\widetilde{\boldsymbol{s}}_4 + \boldsymbol{\alpha}_{3,j}\widetilde{\boldsymbol{s}}_1 + \boldsymbol{n}_3^j \tag{2.1.27}$$

$$\boldsymbol{r}_4^j = -\boldsymbol{\alpha}_{1,j}\widetilde{\boldsymbol{s}}_4 - \boldsymbol{\alpha}_{2,j}\widetilde{\boldsymbol{s}}_3 + \boldsymbol{\alpha}_{3,j}\widetilde{\boldsymbol{s}}_2 + \boldsymbol{n}_4^j \tag{2.1.28}$$

$$\boldsymbol{r}_5^j = \boldsymbol{\alpha}_{1,j}\widetilde{\boldsymbol{s}}_1^* + \boldsymbol{\alpha}_{2,j}\widetilde{\boldsymbol{s}}_2^* + \boldsymbol{\alpha}_{3,j}\widetilde{\boldsymbol{s}}_3^* + \boldsymbol{n}_5^j \tag{2.1.29}$$

$$\boldsymbol{r}_6^j = -\boldsymbol{\alpha}_{1,j}\widetilde{\boldsymbol{s}}_2^* + \boldsymbol{\alpha}_{2,j}\widetilde{\boldsymbol{s}}_1^* - \boldsymbol{\alpha}_{3,j}\widetilde{\boldsymbol{s}}_4^* + \boldsymbol{n}_6^j \tag{2.1.30}$$

$$\boldsymbol{r}_7^j = -\boldsymbol{\alpha}_{1,j}\widetilde{\boldsymbol{s}}_3^* + \boldsymbol{\alpha}_{2,j}\widetilde{\boldsymbol{s}}_4^* + \boldsymbol{\alpha}_{3,j}\widetilde{\boldsymbol{s}}_1^* + \boldsymbol{n}_7^j \tag{2.1.31}$$

$$\boldsymbol{r}_8^j = -\boldsymbol{\alpha}_{1,j}\widetilde{\boldsymbol{s}}_4^* - \boldsymbol{\alpha}_{2,j}\widetilde{\boldsymbol{s}}_3^* + \boldsymbol{\alpha}_{3,j}\widetilde{\boldsymbol{s}}_2^* + \boldsymbol{n}_8^j \tag{2.1.32}$$

Using (2.1.21) through (2.1.24) and (2.1.25) through (2.1.32)

$$\hat{\boldsymbol{s}}_1 = 2\sum_{j=1}^{N_R}[(|\boldsymbol{\alpha}_{1,j}|^2 + |\boldsymbol{\alpha}_{2,j}|^2 + |\boldsymbol{\alpha}_{3,j}|^2)\widetilde{\boldsymbol{s}}_1$$
$$+ \boldsymbol{\alpha}_{1,j}^*\boldsymbol{n}_1^j + \boldsymbol{\alpha}_{2,j}^*\boldsymbol{n}_2^j + \boldsymbol{\alpha}_{3,j}^*\boldsymbol{n}_3^j + \boldsymbol{\alpha}_{1,j}(\boldsymbol{n}_5^j)^* + \boldsymbol{\alpha}_{2,j}(\boldsymbol{n}_6^j)^* + \boldsymbol{\alpha}_{3,j}(\boldsymbol{n}_7^j)^*]$$

$$\hat{\boldsymbol{s}}_2 = 2\sum_{j=1}^{N_R}[(|\boldsymbol{\alpha}_{1,j}|^2 + |\boldsymbol{\alpha}_{2,j}|^2 + |\boldsymbol{\alpha}_{3,j}|^2)\widetilde{\boldsymbol{s}}_2$$
$$+ \boldsymbol{\alpha}_{2,j}^*\boldsymbol{n}_1^j - \boldsymbol{\alpha}_{1,j}^*\boldsymbol{n}_2^j + \boldsymbol{\alpha}_{3,j}^*\boldsymbol{n}_4^j + \boldsymbol{\alpha}_{2,j}(\boldsymbol{n}_5^j)^* + \boldsymbol{\alpha}_{1,j}(\boldsymbol{n}_6^j)^* + \boldsymbol{\alpha}_{3,j}(\boldsymbol{n}_8^j)^*]$$

$$\hat{\boldsymbol{s}}_3 = 2\sum_{j=1}^{N_R}[(|\boldsymbol{\alpha}_{1,j}|^2 + |\boldsymbol{\alpha}_{2,j}|^2 + |\boldsymbol{\alpha}_{3,j}|^2)\widetilde{\boldsymbol{s}}_3$$

$$+\boldsymbol{\alpha}_{3,j}^{*}\boldsymbol{n}_1^j-\boldsymbol{\alpha}_{1,j}^{*}\boldsymbol{n}_3^j-\boldsymbol{\alpha}_{2,j}^{*}\boldsymbol{n}_4^j+\boldsymbol{\alpha}_{3,j}(\boldsymbol{n}_5^j)^*-\boldsymbol{\alpha}_{1,j}(\boldsymbol{n}_7^j)^*-\boldsymbol{\alpha}_{2,j}(\boldsymbol{n}_8^j)^*]$$

$$\hat{\boldsymbol{s}}_4=2\sum_{j=1}^{N_R}[(|\boldsymbol{\alpha}_{1,j}|^2+|\boldsymbol{\alpha}_{2,j}|^2+|\boldsymbol{\alpha}_{3,j}|^2)\widetilde{\boldsymbol{s}}_4$$

$$+\boldsymbol{\alpha}_{3,j}^{*}\boldsymbol{n}_2^j+\boldsymbol{\alpha}_{2,j}^{*}\boldsymbol{n}_3^j-\boldsymbol{\alpha}_{1,j}^{*}\boldsymbol{n}_4^j-\boldsymbol{\alpha}_{3,j}(\boldsymbol{n}_6^j)^*+\boldsymbol{\alpha}_{2,j}(\boldsymbol{n}_7^j)^*-\boldsymbol{\alpha}_{1,j}(\boldsymbol{n}_8^j)^*]$$

it is seen how diversity helps in improving performance. If the channels between the transmit and the receive antennas are assumed to be uncorrelated there is a good likelihood of having some strong signals even if the others are in a deep fade. We see that each transmitted symbol $\widetilde{s}_i, i=1,2,3,4$ is strengthened by all the $3\times N_R$ possible channel coefficients thus giving a maximum diversity order.

### *2.4.3 Simulation results for the quasi-static channel*

The block diagram that illustrates the simulation methodology for $N_T$ transmit antennas and *one* receive antenna is shown below

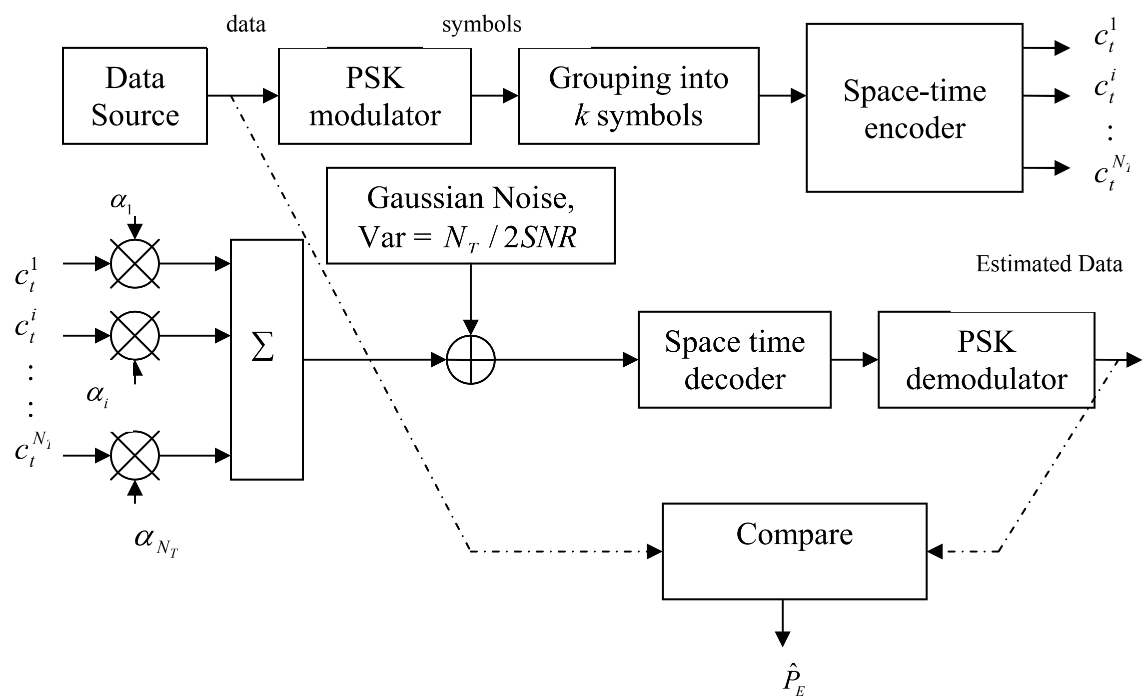


**Fig 2. 3:** System block diagram used for simulations

All simulations assume that the energy of the transmitted symbols is unity. Only one receive antenna is considered in these simulations.

The following plot illustrates the performance of 1 b/s/Hz space-time block-coding scheme in flat Rayleigh fading quasi-static channel. Fading is assumed to be un-correlated.

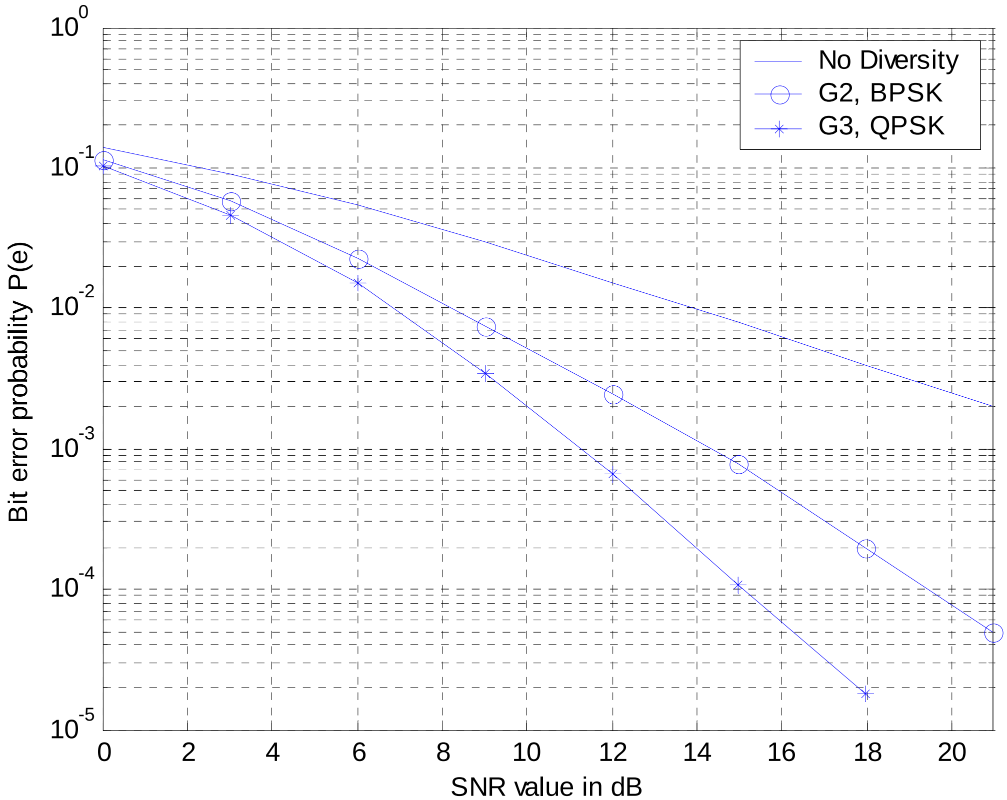


**Fig 2. 4:** BER performance of space-time block codes at 1 bits/s/Hz (1,2 and 3 Transmit antennas)

The following plot illustrates the performance of 2 b/s/Hz space-time block-coding scheme in flat Rayleigh fading quasi-static channel. Fading is assumed to be un-correlated.

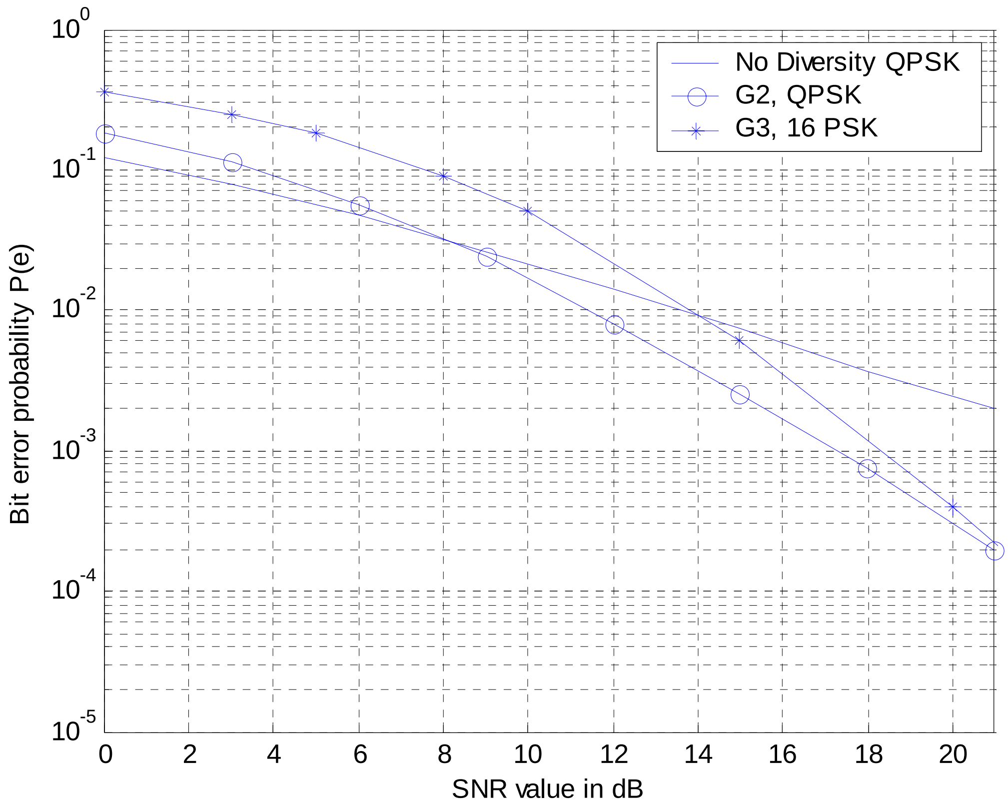


**Fig 2. 5:** BER performance of space-time block codes at 2 bits/s/Hz (1,2 and 3 Transmit antennas)

The following plot illustrates the performance of 3 b/s/Hz space-time block-coding scheme in flat Rayleigh fading quasi-static channel. Fading is assumed to be un-correlated.

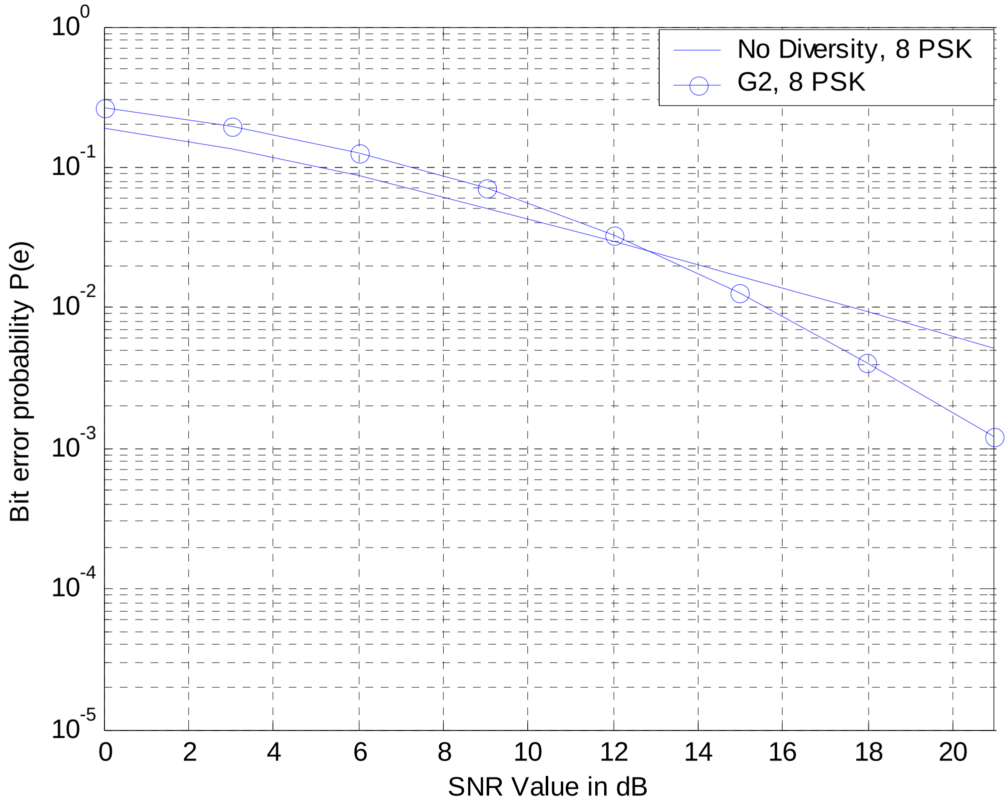


**Fig 2. 6:** BER performance of space-time block codes at 3 bits/s/Hz (1,2 Transmit antennas)

From these simulations we can see that the performance improves as the number of transmit antennas increases. It is observed that as the number of transmit antennas increases, the slope of the BER curves also increases showing that the increase in the number of transmit antennas increases the diversity order of the space-time coded system.

### *2.4.4 Simulation results for the non quasi-static channel*

The following subsections illustrate the results obtained while simulating the space-time codes in a non quasi-static channel with

1. the receiver assuming the channel to be quasi-static and
2. the receiver perfectly estimating all the time varying channel coefficients

Simulations are done at 15 K symbols per second. Flat Rayleigh fading is assumed.

*2.4.4.1 Receiver assumes the channel to be quasi-static*

The following plot illustrates the performance of space-time block codes for a Rayleigh non quasi-static fading channel. The receiver processing is the same as that for a quasi-static channel. The receiver can perfectly estimate the set of channel coefficients associated with the transmission of symbols at $t = 0$. The receiver assumes the same coefficients throughout the length of the frame.

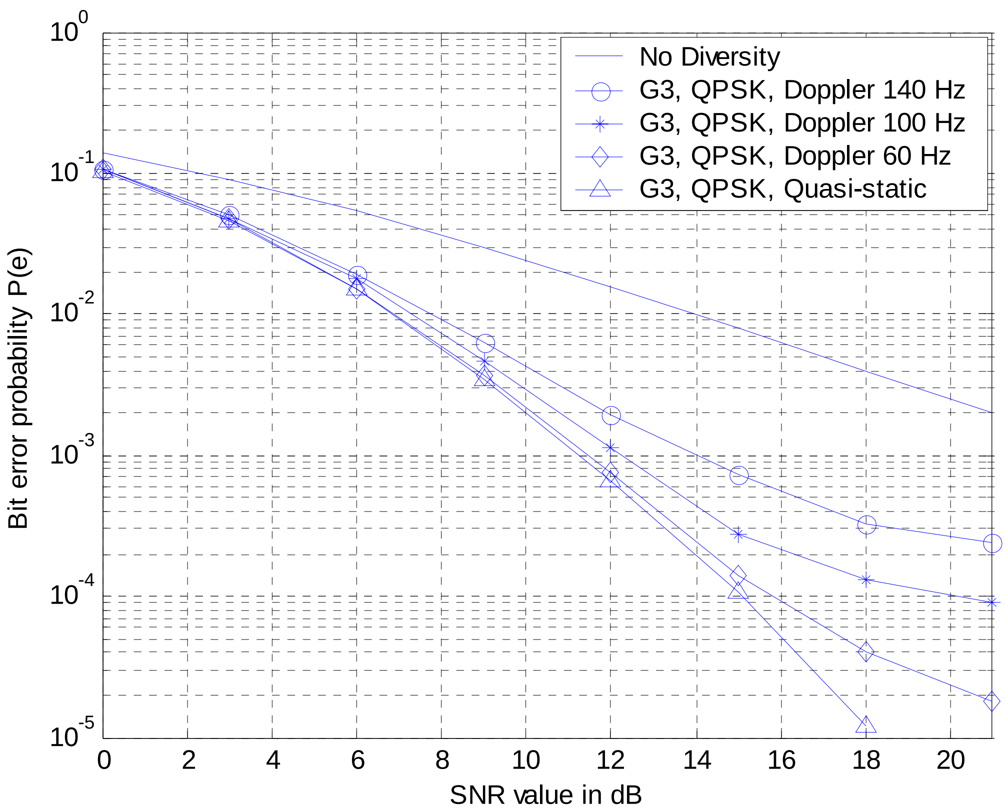


**Fig 2. 7:** BER performance of space-time block codes at 1 bits/s/Hz. Receiver assumes the channel to be quasi-static.

Simulation results show that the performance degrades as the Doppler increases. The receiver however maintains a simple structure as it still assumes quasi-static behavior for the channel. The quasi-static assumption leads to the decoupling of individual symbols to be detected and therefore a lower processing burden at the receiver. The cost of keeping the receiver simple is seen as degradation in performance with increasing Doppler.

*2.4.4.2 The receiver perfectly estimates all time varying channel coefficients within a frame.*

Fig 2.8 illustrates the performance of space-time block codes for a Rayleigh non quasi-static fading channel. The receiver estimates all channel coefficients perfectly and decodes the symbols by minimizing

$$\sum_{t=1}^{p}\sum_{j=1}^{N_R}\left| \boldsymbol{r}_t^j - \sum_{i=1}^{N_T} \boldsymbol{\alpha}_{i,j}^t \boldsymbol{c}_t^i \right|^2 \tag{2.1.33}$$

Notice that (2.1.33) is different from (2.1.16) in that $\boldsymbol{\alpha}_{i,j}$ is replaced by $\boldsymbol{\alpha}_{i,j}^t$ to indicate time varying channel coefficients.

For decoding, the receiver has to minimize the metric given by (2.1.33) for all possible code word sequences $c_1^1 c_1^2 .....c_1^{N_T} c_2^1 c_2^2 .....c_2^{N_T} .....c_p^1 c_p^2 .....c_p^{N_T}$ . Since the Rayleigh coefficients are no longer assumed constant for a frame length, (2.1.33) cannot be decoupled into separate variables as in the quasi-static case. This means that the computational burden for the decoder increases rapidly with increasing transmitter antennas and higher modulation schemes. As an example consider code $G_2$ and one receive antenna. For QPSK, (2.1.33) needs to be computed 16 times to decode 2 symbols. For 8PSK, (2.1.33) needs to be computed 64 times to decode 3 symbols. Again consider code $G_3$ and one receive antenna. For QPSK, (2.1.25) needs to be computed 256 times to decode 4 symbols. For 8PSK, (2.1.25) needs to be computed 4096 times to decode 4 symbols. In general $(m \times m \times m..... \times m)_k$ gives us the number of times (2.1.33) needs to be computed for *m*PSK (or *m*QAM) and *k* transmitted symbols per frame.

Fig 2.8 shows that Doppler does not deteriorate the performance of the space-time code.

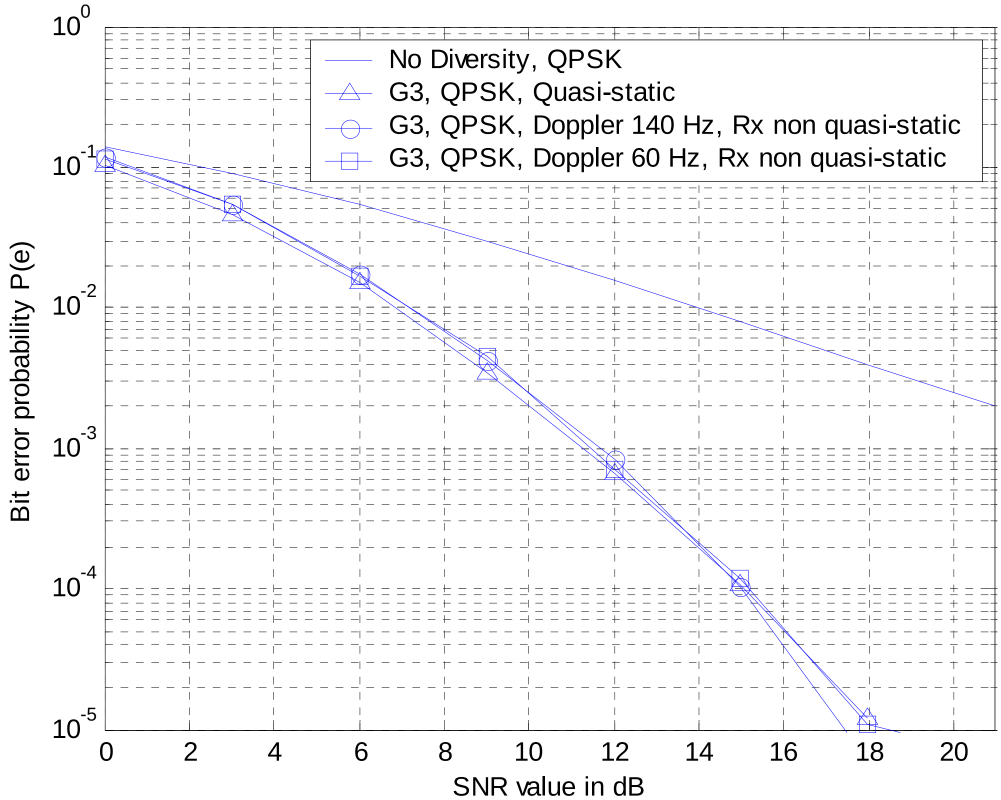


**Fig 2. 8:** BER performance of space-time block codes at 1 bits/s/Hz. Receiver is non quasi-static and estimates all channel coefficients perfectly

It is very unlikely that the receiver can estimate all the channel coefficients perfectly. Simulations were done in which the receiver could perfectly estimate only one set of channel coefficients per frame and all the remaining coefficients were linear interpolation of the perfectly estimated coefficients of two time-adjacent frames. The receiver complexity for such a scheme however still remains the same as that for the previous case.

For the simulation results shown below, code $G_3$ with one receive antenna is used. Consider the first and the second transmitted frame. The simulation assumes that the receiver can perfectly estimate $(\alpha_1^1)^1$, $(\alpha_2^1)^1$ and $(\alpha_3^1)^1$ from the first block and $(\alpha_1^1)^2, (\alpha_2^1)^2$ and $(\alpha_3^1)^2$ from the second block, where the number on the top of the braces represents the block number. All the other channel coefficients in the first block, i.e. $[(\alpha_1^2)^1, (\alpha_2^2)^1, (\alpha_3^2)^1, (\alpha_1^3)^1, (\alpha_2^3)^1, (\alpha_3^3)^1, ....]$ are estimated using the above mentioned perfectly known channel coefficients. The same is done for all other blocks. This is illustrated in the following figure.

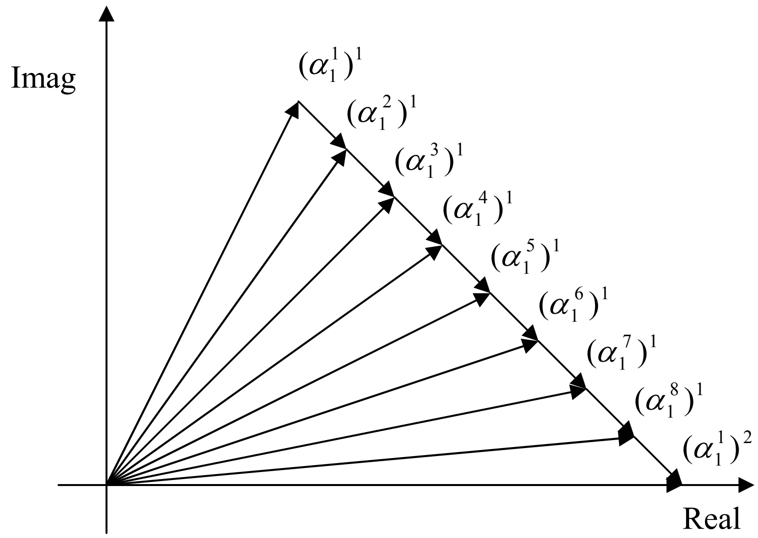


**Fig 2. 9**: Finding channel coefficients by interpolation.

The figure below shows the results of such a simulation.

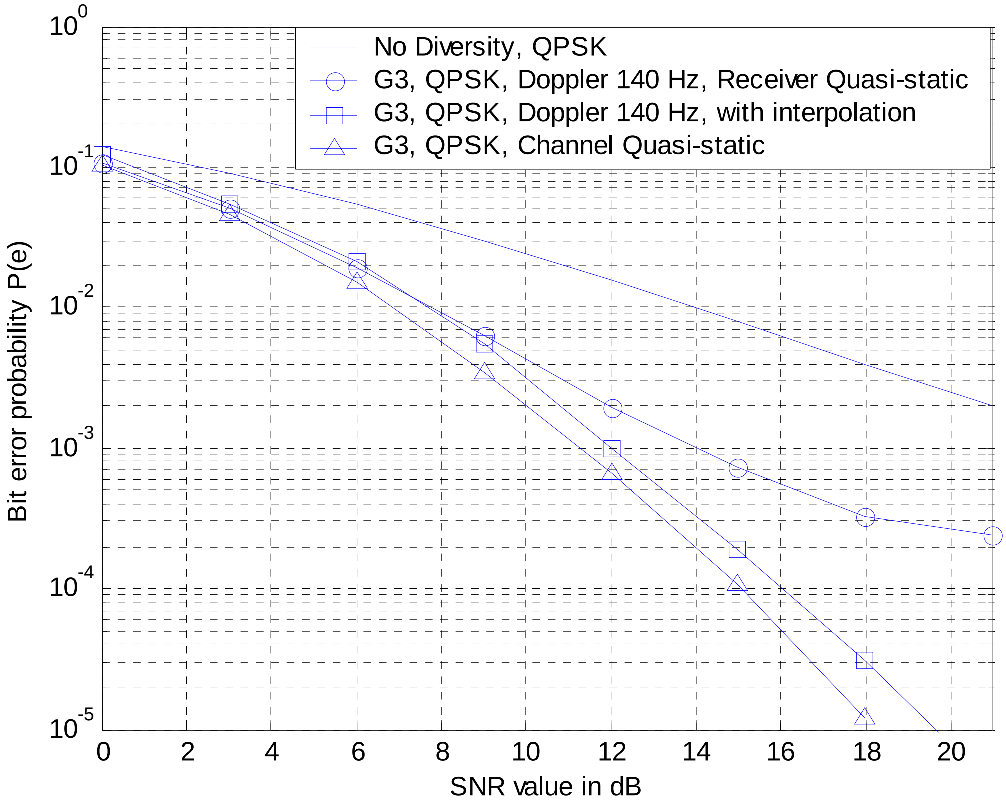


**Fig 2. 10:** BER performance of space-time block codes at 1 bits/s/Hz. Effect of interpolation on performance

Simulation results show that the degradation in performance for the interpolated case is much lower that the quasi-static receiver case.

## *2.5 Summary*

Space-time block codes improve the performance of communication systems by introducing transmit diversity. This chapter introduces the reader to the basic concepts of space-time block coding schemes and provides simulation results for its BER performance.

The best thing about space-time block codes is its simplicity. For quasi-static or a slow fading channel the receiver processing reduces to symbol-by-symbol ML detection. However at high Doppler, performance degrades if the receiver still assumes a quasi-static behavior so as to remain simple. The non quasi-static receiver on the other hand requires significant signal processing to decode symbols.

It is also not practical to assume that all the channel coefficients can be estimated perfectly for a fast fading channel. Simulations that show the performance of space-time block codes if only some of the channel coefficients are estimated perfectly with the others using interpolation estimates do not show a significant degradation in performance.

# Chapter 3

## Concatenated space-time block codes

### 3.1 Introduction

This chapter introduces concatenation schemes for space-time block codes with convolutional codes. First bounds for the bit error performance of space-time block codes in a flat Rayleigh quasi-static channel are derived. The results of this derivation are used in determining the analytical expressions for the error performance of convolutionally concatenated space-time block coding (CCSBC) schemes. Simulation results that verify the validity and tightness of the analytical results are also presented. Improvement in the diversity gain with hard and soft decision decoding for CCSBC system is discussed.

### 3.2 Performance analysis of space-time block codes

In this section we derive bounds for the bit error probability of space-time block codes. Consider a $N_T$ transmit antenna and one receive antenna space-time block coded system. Using (2.1.16) the decision metric for such a system is given by

$$\sum_{t=1}^{p}\left|\boldsymbol{r}_t^{\,j}-\sum_{i=1}^{N_T}\boldsymbol{\alpha}_{i,j}\boldsymbol{c}_t^{\,i}\right|^2 \tag{3.1}$$

For the generalized orthogonal codes $G_2$, $G_3$, $G_4$, $G_3^{'}$, $G_4^{'}$ and equal energy constellation modulation schemes, (3.1) reduces to

$$|\,\hat{\boldsymbol{s}}-\boldsymbol{s}\,| \tag{3.2}$$

$\hat{\boldsymbol{s}}$ is the estimate for the transmitted symbol after appropriate receive combining. $\boldsymbol{s}\in\boldsymbol{S}$, where $\boldsymbol{S}$ is a set of all possible symbols that can be transmitted. The receiver chooses that $\boldsymbol{s}$ which minimizes the Euclidian distance between $\hat{\boldsymbol{s}}$ and $\boldsymbol{s}$.

Let $\tilde{\boldsymbol{s}}_1$ be a symbol transmitted. Suppose the space-time block code used by the encoder is $G_3$. The receiver estimate for $\tilde{\boldsymbol{s}}_1$ is given by

$$\begin{aligned}\hat{\boldsymbol{s}}_1 &= 2(|\boldsymbol{\alpha}_1|^2 + |\boldsymbol{\alpha}_2|^2 + |\boldsymbol{\alpha}_3|^2)\tilde{\boldsymbol{s}}_1 \\ &\quad + \boldsymbol{\alpha}_1^*\boldsymbol{n}_1 + \boldsymbol{\alpha}_2^*\boldsymbol{n}_2 + \boldsymbol{\alpha}_3^*\boldsymbol{n}_3 + \boldsymbol{\alpha}_1(\boldsymbol{n}_5)^* + \boldsymbol{\alpha}_2(\boldsymbol{n}_6)^* + \boldsymbol{\alpha}_3(\boldsymbol{n}_7)^* \qquad (3.3)\end{aligned}$$

The signal energy for $\hat{\boldsymbol{s}}_1$ is given by $4(|\boldsymbol{\alpha}_1|^2 + |\boldsymbol{\alpha}_2|^2 + |\boldsymbol{\alpha}_3|^2)^2$. Let $\boldsymbol{\Theta}$ represents the noise vector for the receiver estimate. From (3.3), $\boldsymbol{\Theta}$ is given by

$$\boldsymbol{\Theta} = \boldsymbol{\alpha}_1^*\boldsymbol{n}_1 + \boldsymbol{\alpha}_2^*\boldsymbol{n}_2 + \boldsymbol{\alpha}_3^*\boldsymbol{n}_3 + \boldsymbol{\alpha}_1(\boldsymbol{n}_5)^* + \boldsymbol{\alpha}_2(\boldsymbol{n}_6)^* + \boldsymbol{\alpha}_3(\boldsymbol{n}_7)^* \qquad (3.4)$$

Its variance can be calculated as

$$\sigma_\Theta^2 = \boldsymbol{E}(\boldsymbol{\Theta}\boldsymbol{\Theta}^*) = 2\sum_{i=1}^{N_T} |\boldsymbol{\alpha}_i|^2 \boldsymbol{E}(\boldsymbol{n}\boldsymbol{n}^*) \ , \qquad N_T = 3 \qquad (3.5)$$

where $\boldsymbol{E}$ is the expectation operator. If $SNR$ is the signal to noise ratio, and $\sigma^2$ is the variance per complex dimension of $\boldsymbol{n}$

$$\boldsymbol{E}(\boldsymbol{n}\boldsymbol{n}^*) = 2\sigma^2 = N_T / SNR, \qquad N_T = 3 \qquad (3.6)$$

Let $\sigma_{\Theta x}^2 = \sigma_{\Theta y}^2$ is the noise variance per complex dimension for the receiver estimate $\hat{\boldsymbol{s}}_1$. Using (3.6) in (3.5) yields

$$\sigma_{\Theta x}^2 = \sigma_{\Theta y}^2 = \frac{2N_T \sum_{i=1}^{N_T} |\boldsymbol{\alpha}_i|^2}{2SNR}, \qquad N_T = 3 \qquad (3.7)$$

In general for codes $G_2$, $G_3$, $G_4$

$$\sigma_{\Theta x}^2 = \sigma_{\Theta y}^2 = \frac{N_T \sum_{i=1}^{N_T} |\boldsymbol{\alpha}_i|^2}{2rSNR} \qquad (3.8)$$

where $r$ is the rate of the code. For codes $G_3^{'}$, $G_4^{'}$ however, (3.8) does not hold good. The variance per complex dimension for these codes can easily be shown to be

$$\sigma_{\Theta x}^2 = \sigma_{\Theta y}^2 = \frac{N_T \sum_{i=1}^{N_T} |\boldsymbol{\alpha}_i|^2}{SNR} \qquad (3.9)$$

Therefore for a general space-time block code we may write

$$\sigma^2_{\Theta x} = \sigma^2_{\Theta y} = K \frac{N_T \sum_{i=1}^{N_T} |\boldsymbol{\alpha}_i|^2}{SNR} \tag{3.10}$$

where $K = \dfrac{1}{2r}$ for $G_2$, $G_3$, $G_4$ and

$= 1$ for $G_3^{'}$, $G_4^{'}$

The decision statistic in general is given by

$$\hat{\boldsymbol{s}} = \frac{1}{b} \sum_{i=1}^{N_T} |\boldsymbol{\alpha}_i|^2 \,\tilde{\boldsymbol{s}} + \boldsymbol{\Theta} \tag{3.11}$$

where $\boldsymbol{\Theta}$ represents Gaussian noise with variance given by (3.10). $b = r$ for $G_2$, $G_3$, $G_4$ and *1* for $G_3^{'}$, $G_4^{'}$. Let $\Omega = \sum_{i=1}^{N_T} |\boldsymbol{\alpha}_i|^2 = \sum_{i=1}^{N_T} \alpha_i^2$ where $\boldsymbol{\alpha}_i = \alpha_i \exp(\phi)$. ML detection is used to estimate $\tilde{\boldsymbol{s}}$ by choosing $\boldsymbol{s}$ that has the minimum distance between the constellation point $\frac{1}{b}\Omega\boldsymbol{s}$ and the receive combining vector $\hat{\boldsymbol{s}}$. The constellation diagram for such an ML receiver and *M-ary PSK* signaling for a given $\Omega$ is shown.

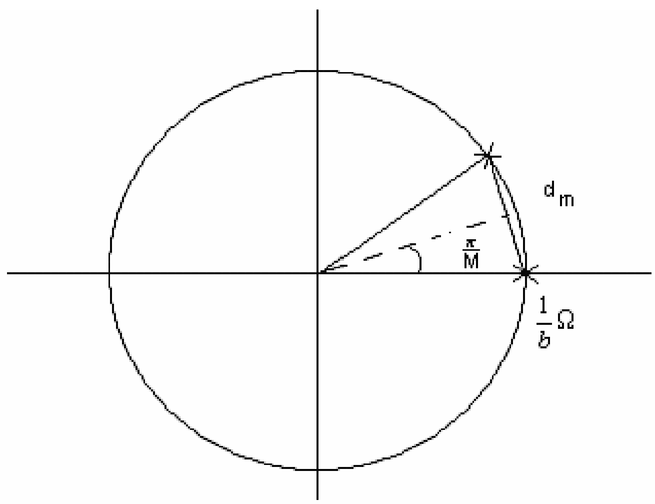


**Fig 3. 1:** Constellation diagram for M-ary PSK space-time decoder

The radius of the circle on which all the possible signals $\frac{1}{b}\Omega\boldsymbol{s}$ lie is given by $\frac{1}{b}\Omega$ for unit energy signals. Using union bound the conditional symbol error probability is given by

$$P(e/\Omega) \le Q\left(\frac{d_m}{2\sigma_{\Theta x}}\right),\ M = 2 \qquad (3.12)$$

$$\le 2Q\left(\frac{d_m}{2\sigma_{\Theta x}}\right),\ M > 2 \qquad (3.13)$$

From fig (3.1),

$$d_m = \frac{2}{b}\Omega \sin(\tfrac{\pi}{M}) \qquad (3.14)$$

Using (3.14) and (3.10) in (3.12) and (3.13)

$$P(e/\Omega) \le AQ\left(\sqrt{\frac{\Omega SNR \sin^2(\frac{\pi}{M})}{b^2 KN_T}}\right) \qquad (3.15)$$

*A* = 1 for *BPSK* and 2 for *M-ary PSK, M > 2.*

Let $E = \dfrac{SNR \sin^2(\frac{\pi}{M})}{b^2 KN_T}$, then

$$P(e/\Omega) \le AQ\left(\sqrt{\Omega E}\right) \qquad (3.16)$$

Since $\alpha$ is Rayleigh distributed, let its *pdf* be given by

$$f_\alpha(\alpha) = \frac{\alpha}{\sigma^2}\exp(-\frac{\alpha^2}{2\sigma^2}) \qquad (3.17)$$

Let $\sigma^2$ be 0.5 i.e. $\boldsymbol{\alpha} = \alpha \exp(\phi)$ is the sum of two orthogonal Gaussian random variables each with 0.5 variance. We are interested in finding the *pdf* of $\alpha^2$. Let $y = g(\alpha) = \alpha^2$. The characteristic function of $y$ is given by

$$\boldsymbol{\Phi}_y = \int_{-\infty}^{\infty} \exp(j\omega y) f_y(y)dy = \boldsymbol{E}\left[\exp(j\omega y)\right] \qquad (3.18)$$

$$= \boldsymbol{E}\left[\exp(j\omega g(\alpha))\right]$$

$$= \int_{-\infty}^{\infty} \exp(j\omega g(\alpha)) f_\alpha(\alpha)d\alpha$$

$$= \int_{-\infty}^{\infty} \exp(j\omega\alpha^2)2\alpha \exp(-\alpha^2)d\alpha$$

$$= \int_{-\infty}^{\infty} \exp(j\omega y)\exp(-y)dy$$

Using the definition of characteristic function from (3.18)

$$f_y(y) = \exp(-y) \tag{3.19}$$

Let

$$\Omega = \alpha_1^2 + \alpha_2^2 + \alpha_3^2 + .......... + \alpha_{N_T}^2$$

$$\Omega = y_1 + y_2 + y_3 + ........... + y_{N_T}$$

Assuming $y_1, y_2, y_3, ........, y_{N_T}$ to be independent, the density of their sum is given by convolution of their densities [12]

$$f_\Omega(\Omega) = f_{y1}(y_1) * f_{y2}(y_2) * f_{y3}(y_3) * ...... * f_{yN_T}(y_{N_T})$$

The characteristic function of $\Omega$ would therefore be given by

$$\boldsymbol{\Phi}_\Omega = \boldsymbol{\Phi}_{y1}\boldsymbol{\Phi}_{y2}\boldsymbol{\Phi}_{y3}......\boldsymbol{\Phi}_{yN_T}$$

Since $y_1, y_2, y_3, ........, y_{N_T}$ are identically distributed

$$\boldsymbol{\Phi}_\Omega = \boldsymbol{\Phi}_y^{N_T} \tag{3.20}$$

The characteristic function of $y$ is

$$\boldsymbol{\Phi}_y(\omega) = \frac{1}{1 - j\omega} \tag{3.21}$$

Using (3.21) in (3.20) yields

$$\boldsymbol{\Phi}_\Omega(\omega) = \frac{1}{(1 - j\omega)^{N_T}} \tag{3.22}$$

This is the characteristic function of a chi-square distributed random variable with $2N_T$ degrees of freedom. Using (2.1-110) from [13]

$$f_\Omega(\Omega) = \frac{\Omega^{N_T - 1}}{(N_T - 1)!}\exp(-\frac{\Omega}{2}), \qquad \Omega > 0 \tag{3.23}$$

The probability of symbol error is given by

$$P(e) = \int_0^{\infty} P(e/\Omega) f_\Omega(\Omega) d\Omega \tag{3.24}$$

Using (3.16), (3.23) in (3.24)

$$P(e) = \int_0^\infty AQ\left(\sqrt{E\Omega}\right)\frac{\Omega^{N_T-1}}{(N_T-1)!}\exp(-\frac{\Omega}{2})d\Omega \tag{3.25}$$

The $Q$ function is defined as [14]

$$Q(z) = \frac{1}{\sqrt{2\pi}}\int_z^\infty \exp(\frac{z^2}{2})dz \tag{3.26}$$

An upper bound for $Q(z)$ is given by

$$Q(z) \le \frac{1}{(\sqrt{2\pi})z}\exp(-\frac{z^2}{2}) \tag{3.27}$$

Using (3.27) in (3.25), the probability of symbol error is given by

$$P(e) \le A\int_0^\infty \frac{1}{\sqrt{2\pi E\Omega}(N_T-1)!}\Omega^{N_T-1}\exp\left(-\frac{(1+E)}{2}\Omega\right)d\Omega$$

$$= \frac{A}{\sqrt{2\pi E}(N_T-1)!}\boldsymbol{I} \tag{3.28}$$

where $\boldsymbol{I}$ is the integral

$$\boldsymbol{I} = \int_0^\infty \frac{\Omega^{N_T-1}\exp\left(-\frac{(1+E)}{2}\Omega\right)}{\sqrt{\Omega}}d\Omega$$

Substituting the transformation $\varphi = \sqrt{\Omega}$

$$\boldsymbol{I} = 2\int_0^\infty \varphi^{2(N_T-1)}\exp\left(-\frac{(1+E)}{2}\varphi^2\right)d\varphi \tag{3.29}$$

This integration has a solution given in appendix G of [11]

$$\boldsymbol{I} = 2^{\frac{2N_T-1}{2}}\frac{\boldsymbol{\Gamma}\left(\frac{2N_T-1}{2}\right)}{(1+E)^{\frac{2N_T-1}{2}}} \tag{3.30}$$

where $\boldsymbol{\Gamma}(*)$ is the gamma function. Some of its properties are

$$\boldsymbol{\Gamma}(n+1) = n\boldsymbol{\Gamma}(n)$$

$$\boldsymbol{\Gamma}(1) = 1 \text{ and } \boldsymbol{\Gamma}(\tfrac{1}{2}) = \sqrt{\pi}$$

Combining (3.28) and (3.30)

$$P(e) \leq \frac{A 2^{\frac{2N_T-1}{2}} \boldsymbol{\Gamma}\left(\frac{2N_T-1}{2}\right)}{\sqrt{2\pi E}(1+E)^{\frac{2N_T-1}{2}}(N_T-1)!} \tag{3.31}$$

(3.31) shows that the diversity order of the single receive, $N_T$ transmit antenna space-time coded system is $N_T$. It can be shown along similar lines that the diversity order would increase to $N_T \times N_R$ if the number of antennas used to receive the signal is increased to $N_R$.

If $b' = \log_2 M$, the probability of bit error assuming mapping of bits into symbols during modulation is Grey coded, is given by

$$P_b(e) \leq \frac{1}{b'} \frac{A 2^{\frac{2N_T-1}{2}} \boldsymbol{\Gamma}\left(\frac{2N_T-1}{2}\right)}{\sqrt{2\pi E}(1+E)^{\frac{2N_T-1}{2}}(N_T-1)!} \tag{3.32}$$

Expressions for BER performance of some space-time coding schemes are summarized below.

1. *G2, BPSK (2 transmit 1 receive antenna, 1 bit/s/Hz space-time block code)*

$$P_b(e) \leq \frac{1}{\sqrt{SNR}(1+SNR)^{3/2}}$$

2. *G3, QPSK (3 transmit 1 receive antenna, 1 bit/s/Hz space-time block code)*

$$P_b(e) \leq \frac{81}{2\sqrt{2SNR}(3+2SNR)^{5/2}}$$

3. *G3, 8PSK (3 transmit 1 receive antenna, 1.5 bits/s/Hz space-time block code)*

$$P_b(e) \leq \frac{1}{\sqrt{0.1953SNR}(1+0.1953SNR)^{5/2}}$$

4. *G2, QPSK (2 transmit 1 receive antenna, 2 bits/s/Hz space-time block code)*

$$P_b(e) \leq \frac{4}{\sqrt{SNR}(1+SNR)^{3/2}}$$

5. *G2, 8PSK (2 transmit 1 receive antenna, 3 bits/s/Hz space-time block code)*

$$P_b(e) \le \frac{2}{3\sqrt{0.1464SNR}(1+0.1464SNR)^{3/2}}$$

Plots that compare the error bounds with simulation results are shown in the following figures

Figure 3.2 shows simulation results and corresponding performance bounds for 1 bit/s/Hz space-time block codes. This figure also shows the performance of un-coded BPSK for comparison purposes.

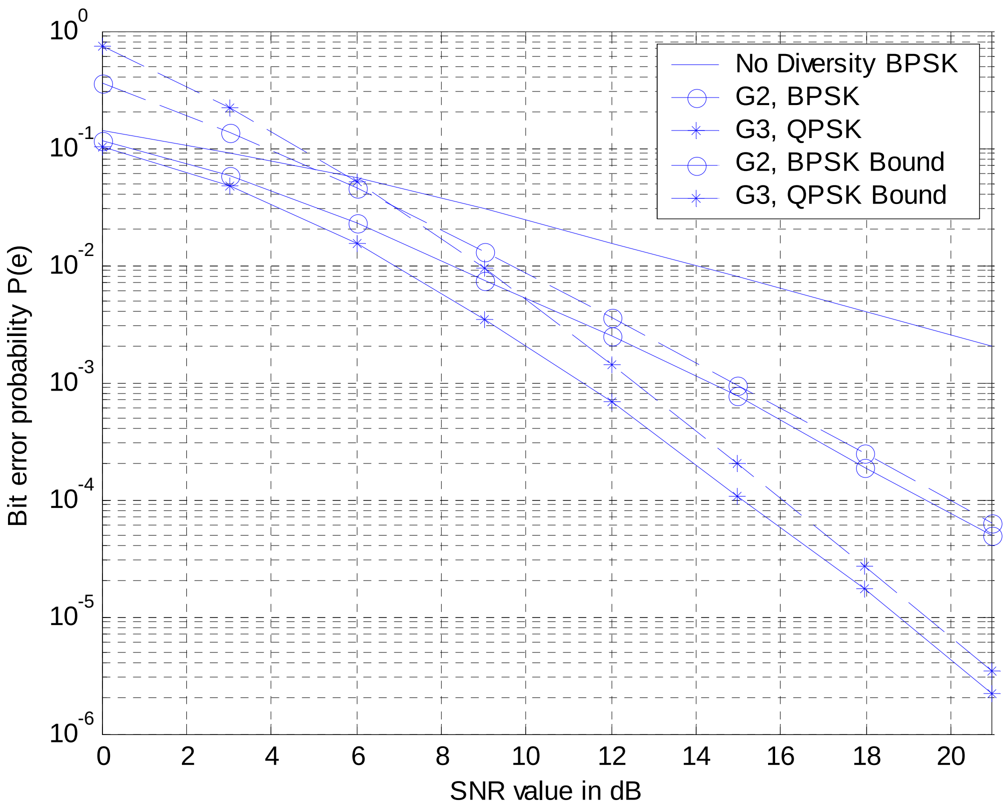


**Fig 3. 2:** Error bounds for 1 bit/s/Hz space-time block codes

Figure 3.3 shows simulation results and corresponding performance bounds for 1.5 and 2 bit/s/Hz space-time block codes. This figure also shows the performance of un-coded QPSK for comparison purposes.

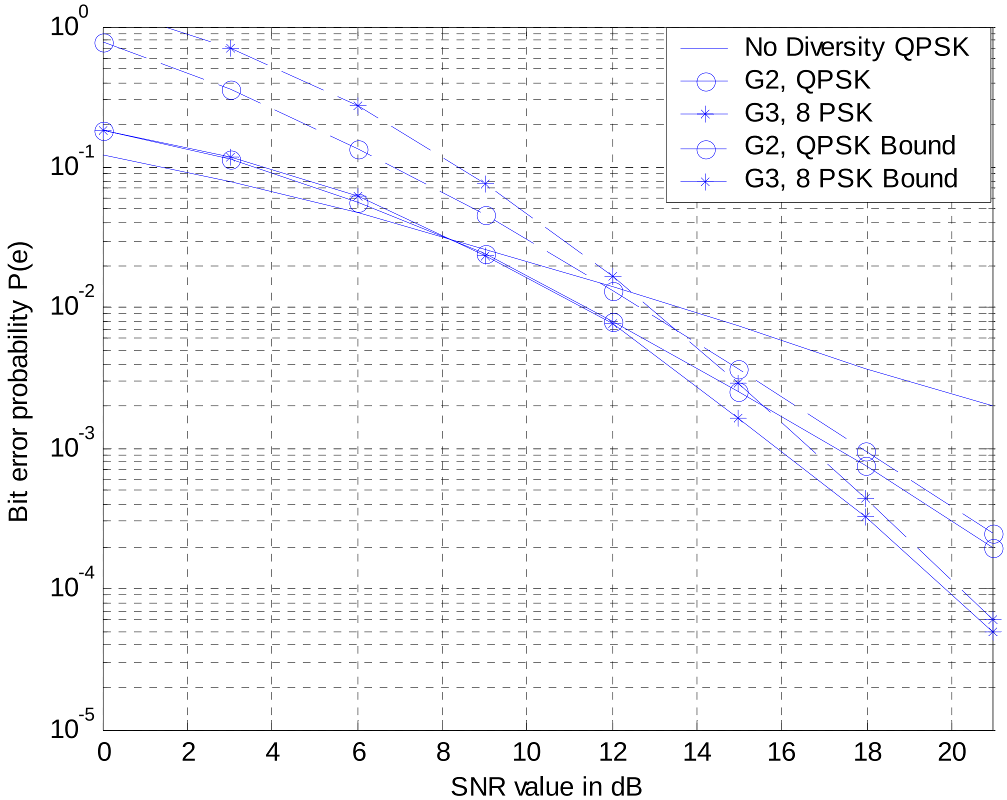


**Fig 3. 3:** Error bounds for 1.5 and 2 bits/s/Hz space-time block codes

Figure 3.4 shows simulation results and corresponding performance bounds for 3 bit/s/Hz space-time block code. This figure also shows the performance of un-coded 8PSK for comparison purposes.

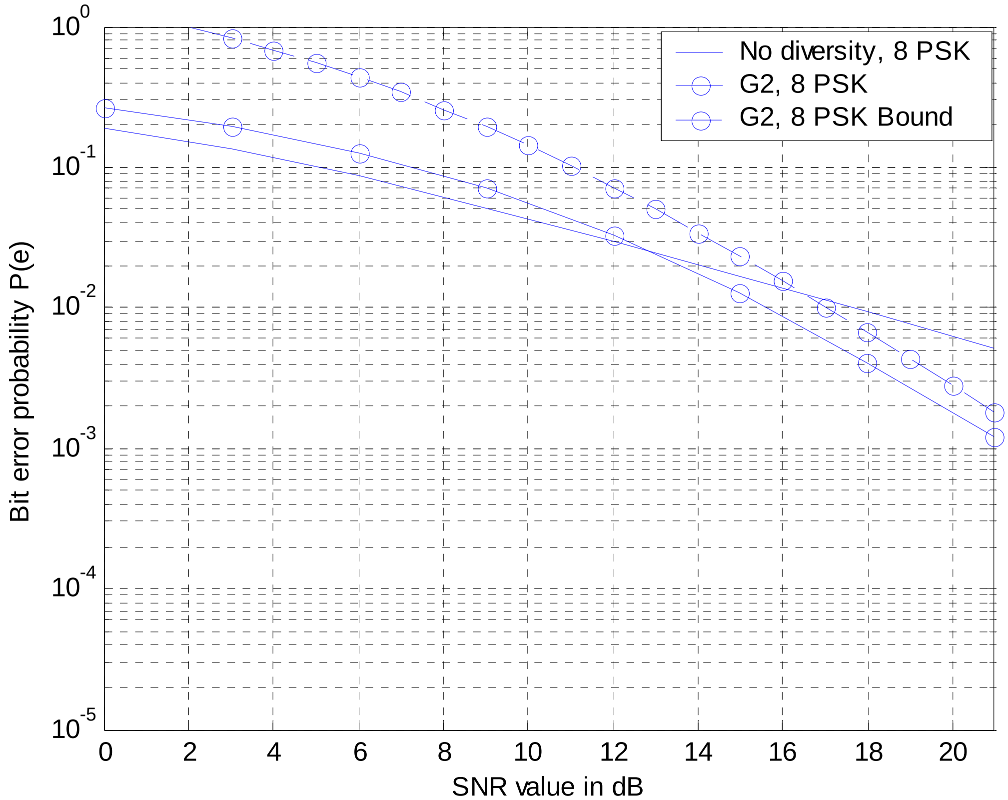


**Fig 3. 4:** Error bounds for 3 bits/s/Hz space-time block codes

## *3.3 Concatenation with convolutional codes*

In this section we discuss convolutional codes and provide simulation results for convolutionally concatenated space-time block coding schemes. Analytical bounds for the schemes discussed are also presented.

### *3.3.1 Convolutional codes*

In this subsection we give a brief introduction to convolutional codes. For a more detailed description, the reader is referred to [15].

A convolutional encoder takes $k$ input bits, passes these through a linear finite state shift register to give $n$ output bits. The rate $R$ of a convolutional code is therefore given by $n/k$. The constraint length $K$ of a convolutional code is defined as the number of bits on which the output depends. There are other definitions of the constraint length where it is defined in k-bit bytes [13] rather than in bits. For each output bit we can associate a generator vector, the elements of which represent the presence or absence of connections from the shift registers to the output. As an example consider the following $R = \frac{1}{2}$ convolutional encoder

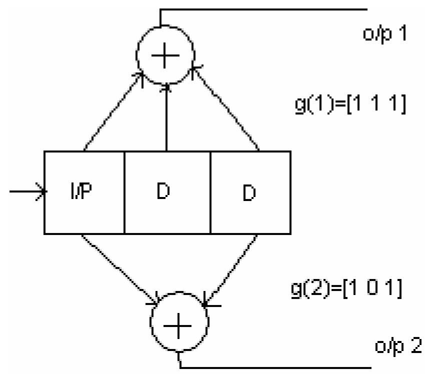


**Fig 3. 5:** Rate one-half, constraint length three convolutional encoder.

The output of the encoder depends upon three input bits, therefore $K = 3$. From the figure we can see that the encoder has two generator vectors given in octal notation as $(7)_8$ and $(5)_8$.

Convolutional codes may be described by tree diagrams, trellis diagrams and state diagrams. Here, we will briefly describe state diagrams. The state of convolutional encoder is given by the contents of the shift register. The state diagram shows all the possible states of a convolutional encoder and all the possible transitions between these states. The state diagram of the $R = \frac{1}{2}$, $K = 3$, generator $[(7)_8,\ (5)_8]$ convolutional encoder is shown in Fig. 3.6

.

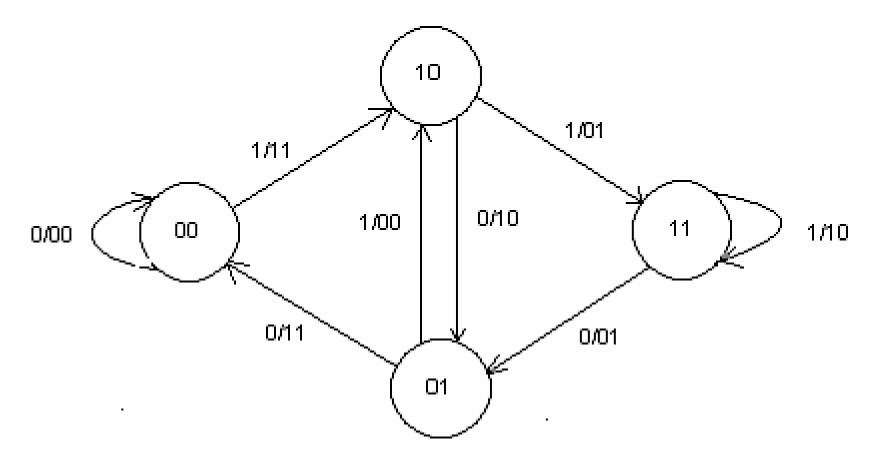


**Fig 3. 6:** State diagram for rate one-half, constraint length 3 convolutional encoder.

In this diagram *x/yz* is interpreted as input *x* results in output *y* at o/p 1 and *z* at o/p 2. The numbers within the circles represent the current state of the encoder.

The error correction and detection performance of convolutional codes depend upon its distance properties. The hamming distance between any two distinct code words is their modulo-2 sum. In other words, it is the number of bits in which the two code words differ. The minimum hamming distance between any two distinct code words is called the free distance $d_f$ of the convolutional code. Better codes have a higher free distance as well as more number of distinct code words at a higher hamming distance.

The state diagram of a convolutional code helps us in finding its transfer function and consequently its distance properties. Let the all-zero sequence be input to the convolutional encoder. The hamming distances from the all-zero sequence to all the other code sequences remain the same even if any sequence other than the all-zero sequence is chosen.

Consider the state diagram in Fig 3.6. Let the all-zero code be the code from which all the distance properties of the particular convolutional code are derived. If the convolutional encoder passes from the states 00-10-01-00, the output of the encoder would be 11-10-11. The distance between the all zero code and this code is 5. Looking at the state diagram, we can see that no other path gives us a distance lower than 5 from the all zero path. The free distance $d_f$ of the code is therefore 5. Counting the number of output ones for all the possible paths starting and ending on the 00 state gives us an indication of all the possible distances and number of codes at a particular distance from the all zero code.

If we label all the branches of the state diagram by $D^n$, where $n$ represents the number of output bits equal to one and find the transfer function with the 00 state as the input and the output of the system, the power of $D$ would give us the distance from the all zero code and the coefficient of $D$ would give the number of codes at that distance. Such a state diagram is shown below.

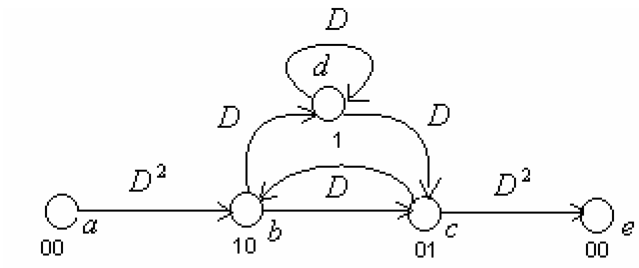


**Fig 3. 7:** State diagram for rate one-half, constraint length three convolutional encoder.

The state equations for the encoder are

$$x_e = D^2 x_c$$

$$x_d = Dx_d + Dx_b$$

$$x_c = Dx_d + Dx_b$$

$$x_b = x_c + D^2 x_a$$

$$T(D) = \frac{x_e}{x_a}$$

$$= \frac{D^2(Dx_d + Dx_b)}{x_a}$$

$$= \frac{D^3(Dx_d + Dx_b) + D^3(x_c + D^2 x_a)}{x_a}$$

$$............$$

$$= D^5 + 2D^6 + 4D^7 + .....$$

From the transfer function we can say that there is one code word with hamming distance five, two code words with hamming distance six and so on. Let us introduce a factor $N$ into those transitions, which are caused by an input bit of 1 [13]. The power of $N$ in the transfer function gives the number of input bits that are 1 for a particular hamming distance given by the corresponding power of *D*. Such a state diagram is given below

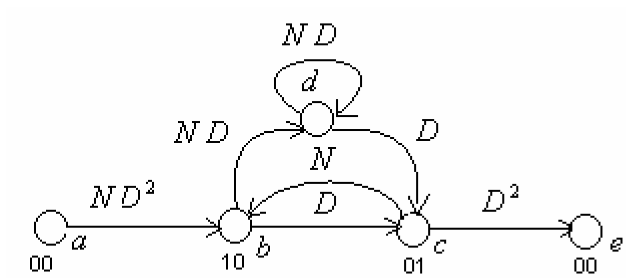


**Fig 3. 8:** State diagram for rate one-half, constraint length three convolutional encoder.

The transfer function is given by

$$T(D,N) = ND^5 + 2N^2D^6 + 4N^3D^7 + \ldots\ldots \tag{3.33}$$

The first term in the transfer function indicates that there is one path at a distance of 5 from the all zero path and of all the bits input to the encoder resulting in this path, only one of the input bits is a 1.

For decoding at the receiver, the most important method used is the Viterbi algorithm. It chooses the code word from the set of all possible code words that has the minimum distance from the received sequence. However, such a choice is not made by searching all the possible code words. Instead, search is done in stages. For the detailed steps involved in the Viterbi algorithm, the reader is referred to [11].

***Hard Decision Decoding***

Consider the following convolutionally encoded system

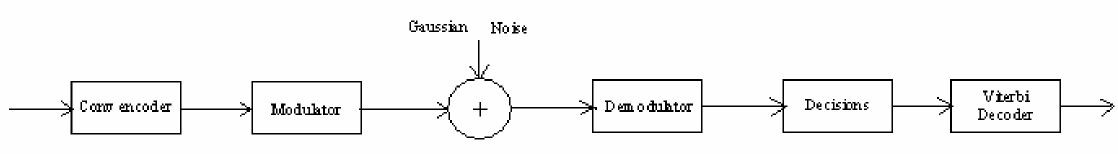


**Fig 3. 9:** Hard decision decoding

After de-modulation hard decisions are made and the output bits are fed into the Viterbi decoder. In order to find the probability of bit error for hard decision decoding, consider a path at a distance $d$ from the transmitted all zero path. The probability of selecting this path instead of the all zero path for hard decision decoding is given by

$$P_2(d) = \sum_{k=(d+1)/2}^{d} \binom{d}{k} p^k (1-p)^{d-k} \tag{3.34}$$

for $d$ odd and

$$P_2(d) = \sum_{k=d/2+1}^{d} \binom{d}{k} p^k (1-p)^{d-k} + 0.5 \binom{d}{\frac{1}{2}d} p^{\frac{d}{2}} (1-p)^{\frac{d}{2}} \tag{3.35}$$

for $d$ even. Here $p$ is the probability of bit error for a binary symmetric channel. $P_2(d)$ is the pair-wise error probability for a particular path at a distance $d$.

A loose but mathematically compact Chernoff upper bound is given by [13]

$$P_2(d) < \left[\sqrt{4p(1-p)}\right]^d \tag{3.36}$$

The first event error probability $P_e$ is defined as the probability that another path in the Viterbi decoder merges with the all zero path for the first time with a metric that is greater than that for the all zero path [13]. An upper bound for the first event probability can be obtained by summing up the pair-wise error probabilities for all the possible paths that can merge with the all zero path. The first event error probability is therefore upper bounded by [13]

$$P_e < \sum_{d=dfree}^{\infty} a_d P_2(d) \tag{3.37}$$

where $a_d$ is the number of paths at a distance $d$ from the all zero path. This number is given by the coefficients of $D^n$ in the expansion of $T(D)$.

Since the exponent of $N$ in the transfer function $T(D,N)$ gives the number of 1's input to the Viterbi decoder when a non zero (or incorrect) path is selected, the probability of bit error is upper bounded by [13]

$$P_b < \sum_{d=dfree}^{\infty} c_d P_2(d) \tag{3.38}$$

where $c_d$ is the coefficient of $D^d$ in the expansion of the derivative of $T(D,N)$ at $N=1$. If the Chernoff bound is used

$$P_b < \left.\frac{dT(D,N)}{dN}\right|_{N=1,D=\sqrt{4p(1-p)}}$$

For a k-input convolutional encoder the probability of bit error for hard decision decoding is given by

$$P_b < \frac{1}{k}\left.\frac{dT(D,N)}{dN}\right|_{N=1,D=\sqrt{4p(1-p)}} \tag{3.39}$$

***Soft Decision Decoding***

Consider the following convolutionally encoded system

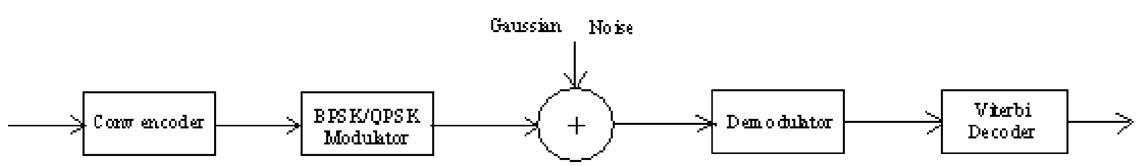


**Fig 3. 10:** Soft decision decoding

The output of the de-modulator is fed into the Viterbi decoder without any prior decisions. Consider BPSK modulation with bits transmitted at unit energy. The pair-wise error probability at a distance $d$ for soft decision decoding is given by

$$P_2(d) = Q\left(\frac{d_m}{2\sigma}\right)$$

where $\sigma$ is the standard deviation per complex dimension of the Gaussian noise and $d_m$ is the Euclidian distance between the two code words. For BPSK without convolutional coding the distance between the two constellation points is $2\sqrt{E_b} = 2$ (assuming transmission bit energy to be unity). Due to convolutional coding the Euclidian distance between two code words at a hamming distance $d$ is increased to $2\sqrt{dE_b} = 2\sqrt{d}$. Therefore the pair-wise error probability is given by

$$P_2(d) = Q\left(\frac{\sqrt{d}}{\sigma}\right) \tag{3.41}$$

Since $\sigma^2 = \frac{1}{2SNR}$, the pair-wise error probability is given by

$$P_2(d) = Q\left(\sqrt{2dSNR}\right) \tag{3.42}$$

The first event error probability is upper bounded by (3.37). Using (3.42) in (3.37) the first event error probability is given by

$$P_e < \sum_{d=dfree}^{\infty} a_d Q(\sqrt{2dSNR}) \tag{3.43}$$

For comparison purposes with un-coded systems code R rate may be introduced in (3.42) and (3.43)

$$P_2(d) = Q\left(\sqrt{2dRSNR}\right) \tag{3.44}$$

$$P_e < \sum_{d=dfree}^{\infty} a_d Q(\sqrt{2dRSNR}) \tag{3.45}$$

The bit error probability for soft decision decoding for a k input convolutional code is therefore given by

$$P_b < \frac{1}{k} \sum_{d=dfree}^{\infty} \left.\frac{dT(D,N)}{dN}\right|_{N=1,D=1} P_2(d) \tag{3.46}$$

$$= \frac{1}{k} \sum_{d=dfree}^{\infty} c_d P_2(d) \tag{3.47}$$

Table 3.1 lists the first three $c_d$ terms $(c_{dfree}, c_{dfree+1}, c_{dfree+2})$ for rate $\frac{1}{2}$ *optimum* convolutional codes.

| $K$ | *Generators (base 8)* | $d_f$ | $c_d$ |
|---|---|---|---|
| 3 | (5,7) | 5 | [1, 4, 12] |
| 5 | (23,35) | 7 | [4, 12, 20] |
| 7 | (133,171) | 10 | [36, 0, 211] |
| 9 | (561,753) | 12 | [33, 0, 50] |

**Table 3. 1:** Rate $\frac{1}{2}$ optimum distance convolutional codes. Source Prenger, P$\overset{o}{a}$l, et al. (1999) [16]



Table 3.2 lists the first three $c_d$ terms $(c_{dfree}, c_{dfree+1}, c_{dfree+2})$ for rate $\frac{1}{3}$ *optimum* convolutional codes.

| $K$ | *Generators (base 8)* | $d_f$ | $c_d$ |
|---|---|---|---|
| 3 | (5, 7, 7) | 8 | [3, 0, 15] |
| 5 | (25,33, 37) | 12 | [12, 0, 12] |
| 7 | (133, 165, 171) | 15 | [7, 8, 22] |
| 9 | (575, 623, 727) | 18 | [2, 10, 50] |

**Table 3. 2:** Rate $\frac{1}{3}$ optimum distance convolutional codes. Source Prenger, P$\overset{o}{a}$l, et al. (1999) [16]



### *3.3.2 Performance of convolutional coded systems in Rayleigh Channel*

Let us first derive an expression for the performance of an un-coded PSK modulated system in Rayleigh fading. The channel coefficients $\boldsymbol{\alpha} = \alpha \exp(\varphi)$ are assumed to be Gaussian with zero mean and 0.5 variance per complex dimension. The receiver is assumed to have perfect knowledge of the channel. The energy of the transmitted symbols is assumed to be unity.

If $\Omega = \alpha^2$ the density of $\Omega$ as shown in (3.19) is given by

$$f_{\Omega}(\Omega) = \exp(-\Omega) \tag{3.48}$$

The conditional probability of symbol error, for known $\Omega$ is given by

$$P(e/\Omega) \le Q\left(\frac{d_m}{2\sigma_{\Theta x}}\right),\ M = 2 \tag{3.49}$$

$$\le 2Q\left(\frac{d_m}{2\sigma_{\Theta x}}\right),\ M > 2 \tag{3.50}$$

where $d_m$ is the minimum Euclidean distance of the decision statistic given by

$$d_m = 2\Omega \sin(\tfrac{\pi}{M}) \tag{3.51}$$

and $\sigma_{\Theta x}^2$ is the noise variance per complex dimension of the decision statistic given by

$$\sigma_{\Theta x} = \sqrt{\Omega/2SNR} \tag{3.52}$$

Using (3.51) and (3.52) in (3.49) and (3.50) we have

$$P(e/\Omega) < Q(\sqrt{2\Omega SNR}),\qquad M = 2 \tag{3.53}$$

$$< 2Q(\sqrt{2\Omega SNR \sin^2 \tfrac{\pi}{M}},\qquad M > 2 \tag{3.54}$$

The probability of error is given by

$$P(e) = \int_{-\infty}^{\infty} P(e/\Omega) f_\Omega(\Omega) d\Omega$$

$$= \int_{0}^{\infty} AQ(\sqrt{2\Omega SNR \sin^2 \tfrac{\pi}{M}}) \exp(-\Omega) d\Omega \tag{3.55}$$

where $A$ is 1 for BPSK and 2 for MPSK. (3.55) has a closed form solution given by

$$P(e) = \frac{A}{2}\left(1 - \sqrt{\frac{SNR \sin^2 \frac{\pi}{M}}{1 + SNR \sin^2 \frac{\pi}{M}}}\right) \tag{3.56}$$

The probability of bit error for a grey coded modulation scheme is given by

$$P_b(e) = \frac{A}{2b'}\left(1 - \sqrt{\frac{SNR \sin^2 \frac{\pi}{M}}{1 + SNR \sin^2 \frac{\pi}{M}}}\right) \tag{3.57}$$

where $b' = \log_2 M$.

For BPSK (3.57) reduces to

$$P_b(e) = \frac{1}{2}\left(1 - \sqrt{\frac{SNR}{1 + SNR}}\right) \tag{3.58}$$

The figure compares the simulation results for BPSK modulation with the analytical result of (3.58)

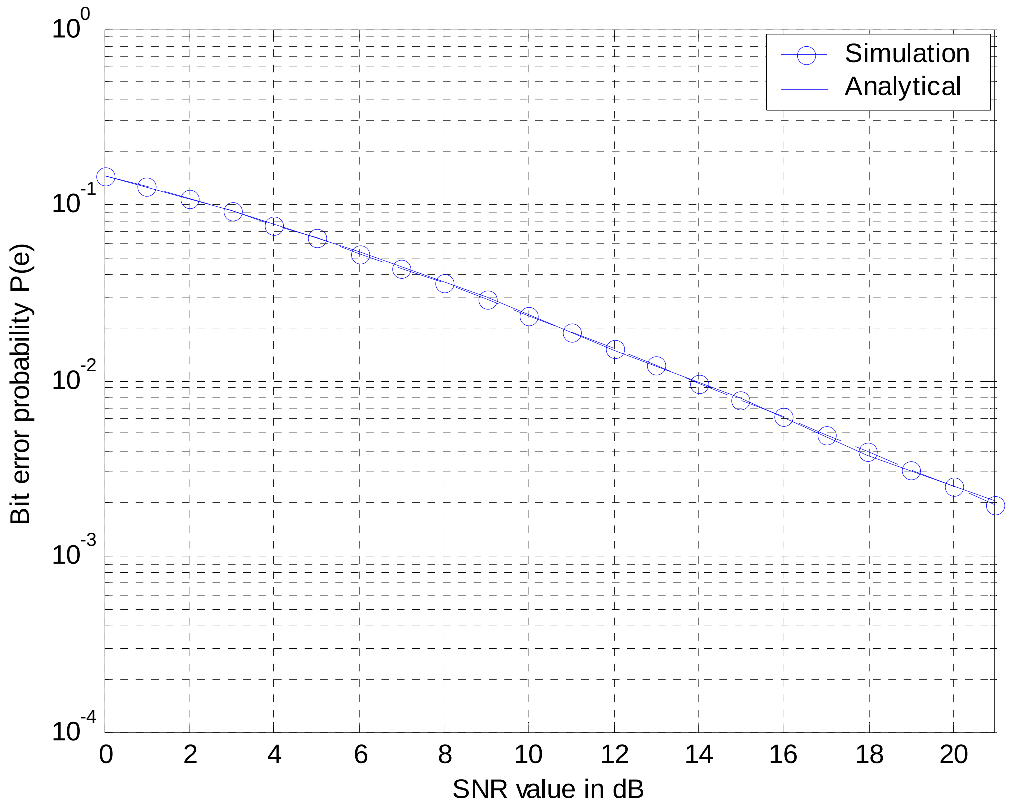


**Fig 3. 11:** Comparison of analytical and simulated performance of BPSK in Rayleigh fading channel of variance of 0.5

Let us now consider a convolutionally coded system in a Rayleigh fading channel. The system block diagram is shown in Fig. (3.12)

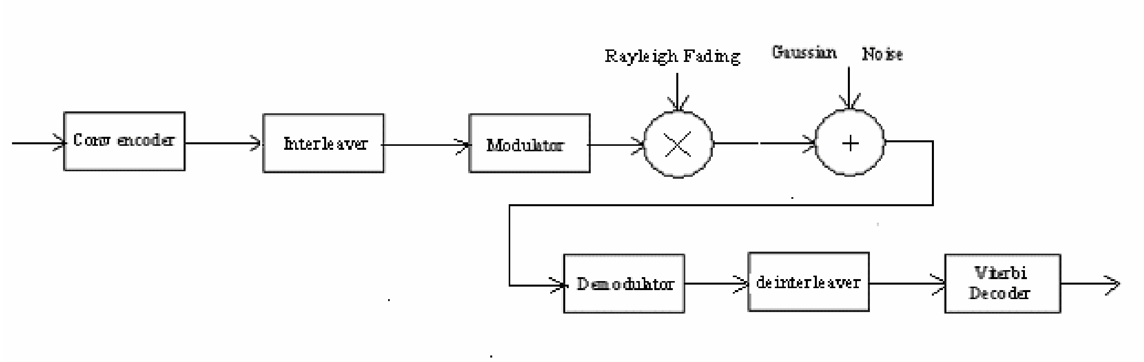


**Fig 3. 12:** Convolutionally coded communication system

In order to make the bursty Rayleigh fading channel have statistically independent errors, interleaving is introduced into the communication system. Consider hard decision decoding first. Let the modulation be BPSK. The probability of bit error is given by (3.38). Using (3.34) and (3.35) in (3.38), the probability of bit error can be obtained. We may assume $p$ approximates $P_b(e)$ given in (3.58) provided an interleaver of sufficient depth (or preferably random) is used.

Fig. (3.13) illustrates simulation results for a constraint length 3, rate 0.5 convolutional encoder with generators $(5)_8$ and $(7)_8$. The interleaving degree for the block interleaver used is taken to be 20. Bits are transmitted at unit energy (without rate compensation). The figure also shows the analytical bound for comparison purposes. The simulation and analytical results are rate uncompensated.

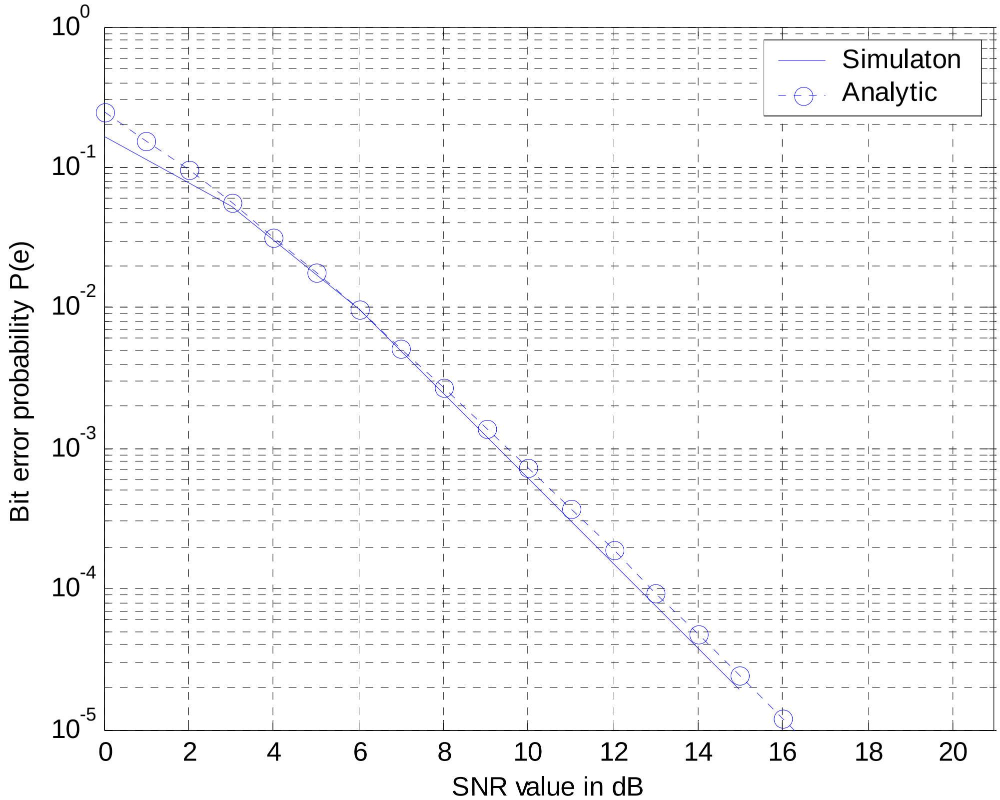


**Fig 3. 13:** Hard decision decoding. Performance of K=3, R = 0.5 convolutional encoder with generators $(5)_8$ and $(7)_8$.

If instead of the exact expression for the pair-wise error probability, the Chernoff bound is used

$$P_b < \sum_{d=dfree}^{\infty} c_d \left(\sqrt{4p(1-p)}\right)^d \tag{3.59}$$

and the probability of bit error is assumed to given by the first term of the expansion of the above sum, using (3.58) we have

$$P_b \approx \left(\frac{1}{1+SNR}\right)^{dfree/2}$$

The diversity provided by hard decision decoding at high *SNRs* is half the free distance.

Now let us consider soft decision decoding. BPSK modulation and perfect interleaving is assumed. The pair-wise error probability between the all zero path and a path at a distance $d$ from it for convolutional codes using soft Viterbi decoding is given by [13]

$$P_2(d) = P\left(\sum_{l=1}^{d} r_l' \geq 0\right) \tag{3.60}$$

where the summation represents the sum of inputs to the decoder for all the $d$ bits which cause the two paths to differ. Let

$$r = \sum_{l=1}^{d} r_l' .$$

For unit energy signals, we may write

$$\boldsymbol{r} = \Omega + \boldsymbol{\Theta}$$

where $\Omega = \sum_{i=1}^{d} |\alpha_i|^2$ and $\boldsymbol{\Theta}$ is the complex Gaussian noise with variance $\frac{\Omega}{2SNR}$ per complex dimension. The probability $r \geq 0$ for known $\Omega$ is given by (3.12), which in our case reduces to

$$P(r \geq 0/\Omega) = Q\left(\sqrt{2\Omega SNR}\right) \tag{3.61}$$

The total probability is given by

$$P(r \geq 0) = \int_0^{\infty} P(r \geq 0/\Omega) f_{\Omega}(\Omega) d\Omega \tag{3.62}$$

Using (3.61) and (3.23) in (3.62) and proceeding along the same lines as in section 3.2, the total probability is calculated as

$$P(r \geq 0) = P_2(d) = \frac{2^{\frac{2d-1}{2}} \boldsymbol{\Gamma}\left(\frac{2d-1}{2}\right)}{\sqrt{4\pi SNR}\,(1+2SNR)^{\frac{2d-1}{2}}\,(d-1)!} \tag{3.63}$$

The probability of bit error can be obtained by using (3.63) in (3.47).

The figure (3.10) compares the performance of soft and hard decision decoding in a Rayleigh fading channel for the constraint length 3, rate 0.5 convolutional codes with generators $(5)_8$ and $(7)_8$. The performance is not rate compensated and perfect interleaving is assumed.

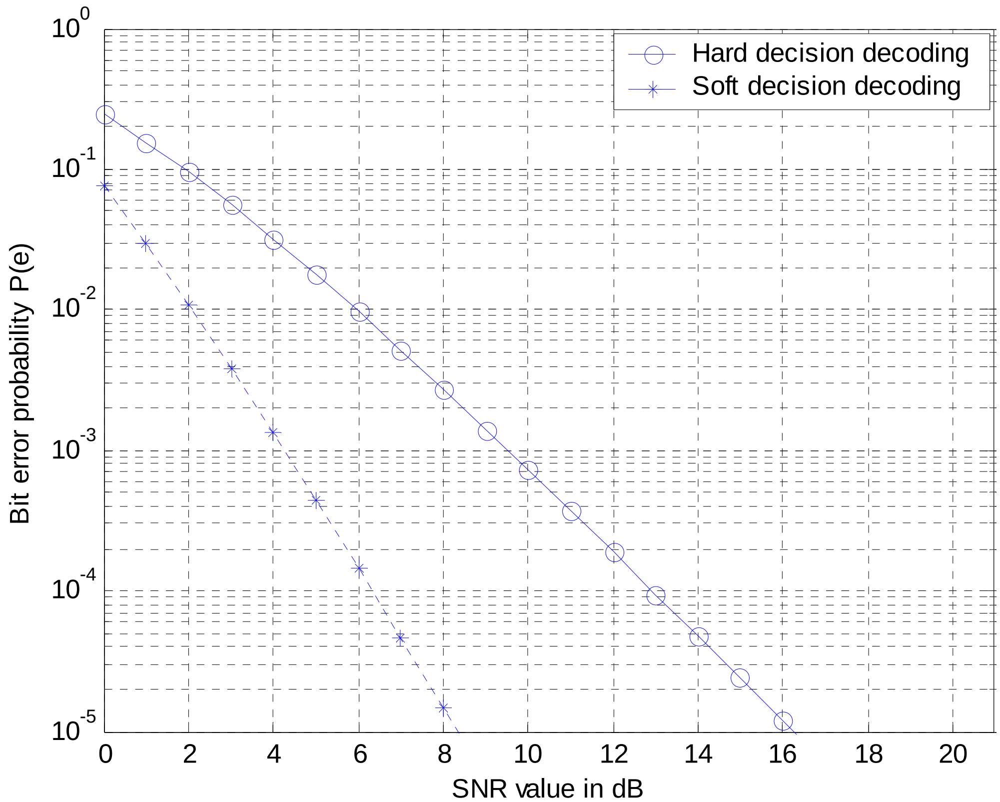


**Fig 3. 14:** Improvement in diversity due to soft decision Viterbi decoding

If the probability of bit error is assumed to given by the first term of the expansion of (3.47)

$$P_b \approx \frac{2^{\frac{2dfree-1}{2}} \boldsymbol{\Gamma}\left(\frac{2dfree-1}{2}\right)}{\sqrt{4\pi SNR}\,(1+2SNR)^{\frac{2dfree-1}{2}}\,(dfree-1)!}$$

At high *SNRs* the diversity provided equals the free distance. Compared to hard decision decoding, soft decision decoding increases the diversity order from $dfree/2$ to $dfree$.

### *3.3.3 Convolutionally concatenated space-time block codes (CCSBC)*

The block diagram showing the convolutionally concatenated space-time block coded system is shown in Fig. 3.15

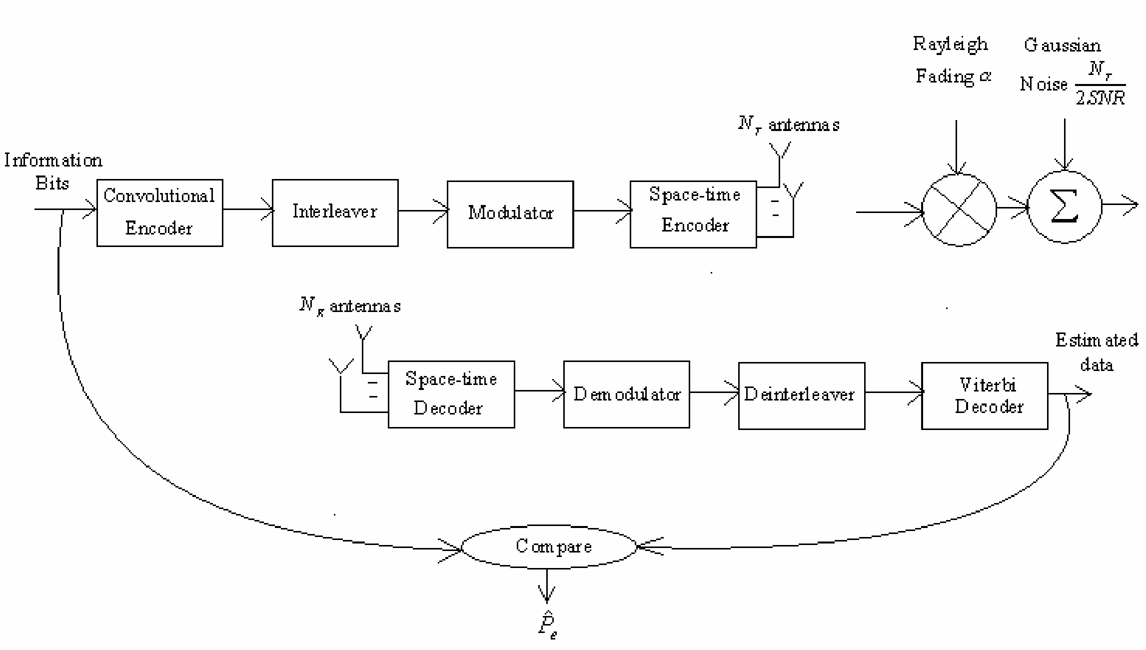


**Fig 3. 15:** Convolutionally concatenated space-time block coded system

Information bits after being encoded by the convolutional encoder are passed through the interleaver. The interleaver randomizes the encoded bits, improving the performance of the communication system in bursty channels. Modulation is performed on the interleaved bits. The modulated bits are then space-time encoded. The transmitted symbols undergo Rayleigh fading as they pass through the channel. At the receiving end of the system, the space-time decoder finds the receive estimates of the input symbols. For hard decision Viterbi decoding these symbols are demodulated and hard decisions are made to give the output bit sequence. For soft decision decoding, soft decisions are made to give output soft bit sequence. The output bit sequence in both cases is de-interleaved and passed through the Viterbi decoder to give the received bits.

***Performance of CCSBC systems with hard decision decoding***

The following plots illustrate the simulation results for the performance of convolutionally concatenated space-time block codes with hard decision decoding. The modulation is assumed to be PSK. The average energy of symbols transmitted is taken to be one. Different space-time block coding schemes have been used. The Rayleigh fading channel is taken to be the sum of two zero mean quadrature Gaussian random variables at a variance of 0.5 per complex dimension. The Gaussian noise added to the system is zero mean with variance $\frac{N_T}{2SNR}$. All simulations assume single receive antenna.

*Half bit per sec per Hz, CCSBC*

Simulation results for half bits/s/Hz CCSBC systems are shown. These are compared with a rate one-half space-time block coded system without concatenated convolutional codes.

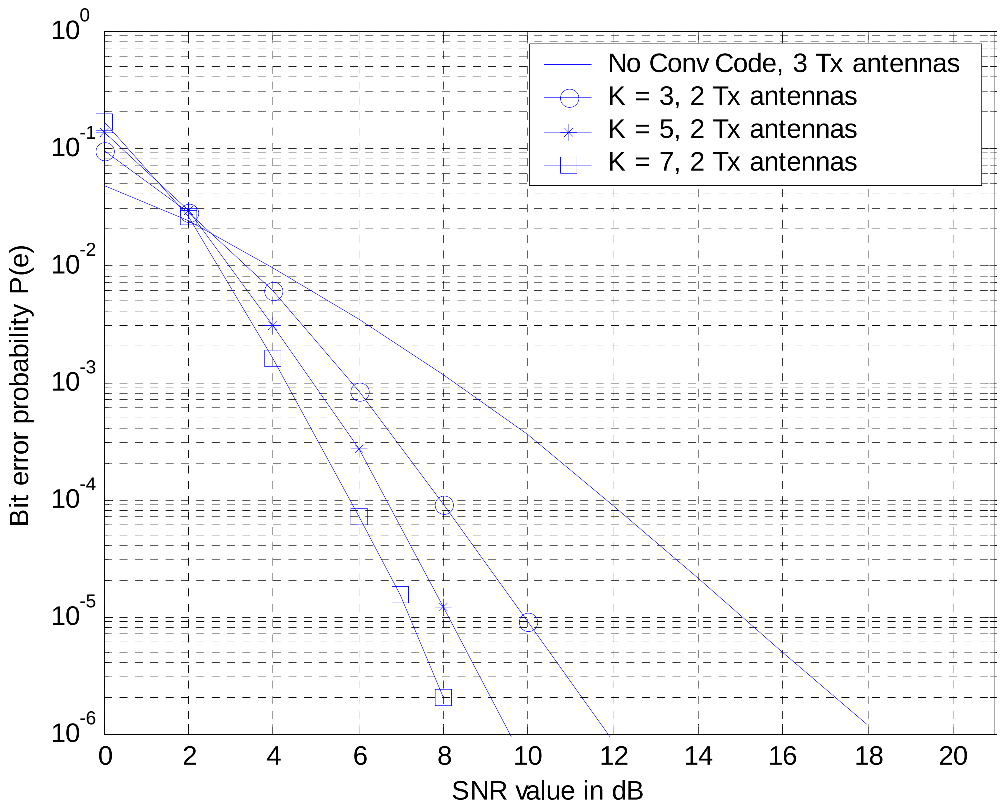


**Fig 3. 16:** Performance of half bits/s/Hz CCSBC systems

The three transmit antenna scheme employs code $G_3$ and uses BPSK modulation. All the convolutionally concatenated systems in this simulation are two transmit antenna schemes, employ code $G_2$ and use BPSK modulation. The convolutional codes used in this simulation are rate one-half and have constraint lengths 3, 5 and 7. These are given in table (3.1). Hard decision decoding is performed. We can see that improving the diversity by using an additional third antenna is not as advantageous as concatenation by convolutional codes for the same overall system rate.

*One bit per sec per Hz, CCSBC*

Simulation results for one bit/s/Hz CCSBC systems are shown. These are compared with a two transmit antenna and a three transmit antenna, rate one space-time block coded system without concatenated convolutional codes.

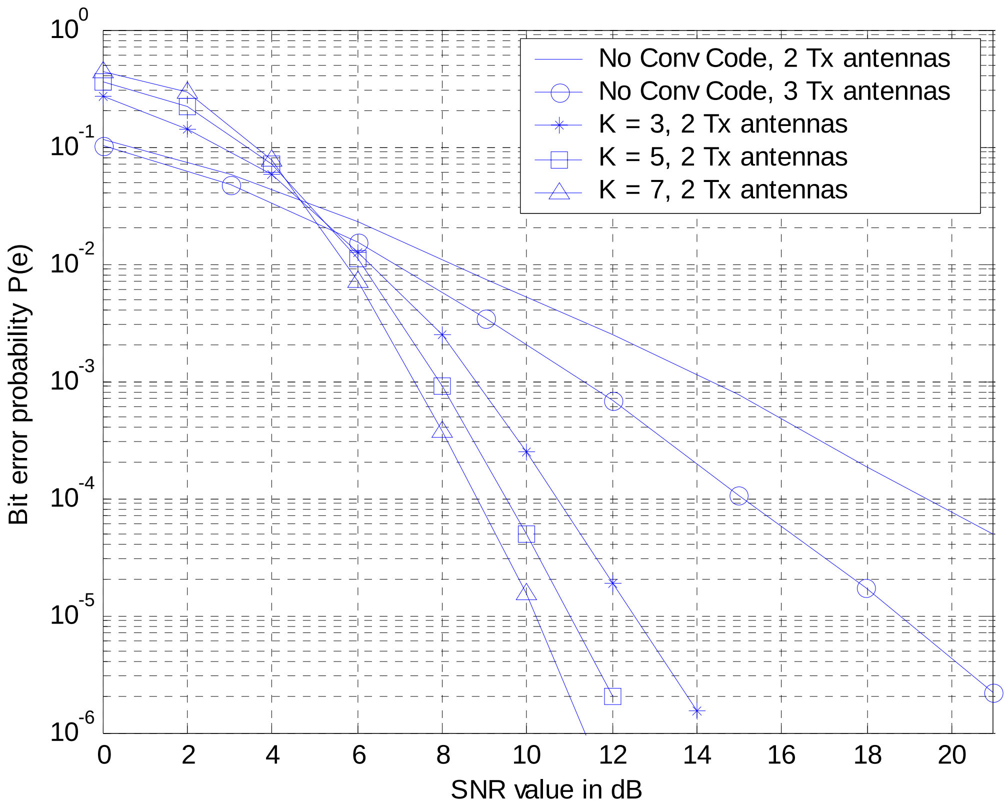


**Fig 3. 17:** Performance of one bits/s/Hz CCSBC systems

The two transmit antenna scheme without the convolutional code employs space-time code $G_2$ and uses BPSK modulation. The three transmit antenna scheme without the convolutional code employs space-time code $G_3$ and uses QPSK modulation. All the convolutionally concatenated systems in this simulation are two transmit antenna schemes, employ code $G_2$ and use QPSK modulation. The convolutional codes used in this simulation are rate one-half and have constraint lengths 3, 5 and 7. These are given in table (3.1). Hard decision decoding is performed. We can see that improving the diversity by using an additional third antenna is not as advantageous compared to concatenation by convolutional codes for the same overall system rate.

*One and a half bit per sec per Hz, CCSBC*

Simulation results for 3/2 bits/s/Hz CCSBC systems are shown. These are compared with a rate 3/2 space-time block coded system without concatenated convolutional codes.

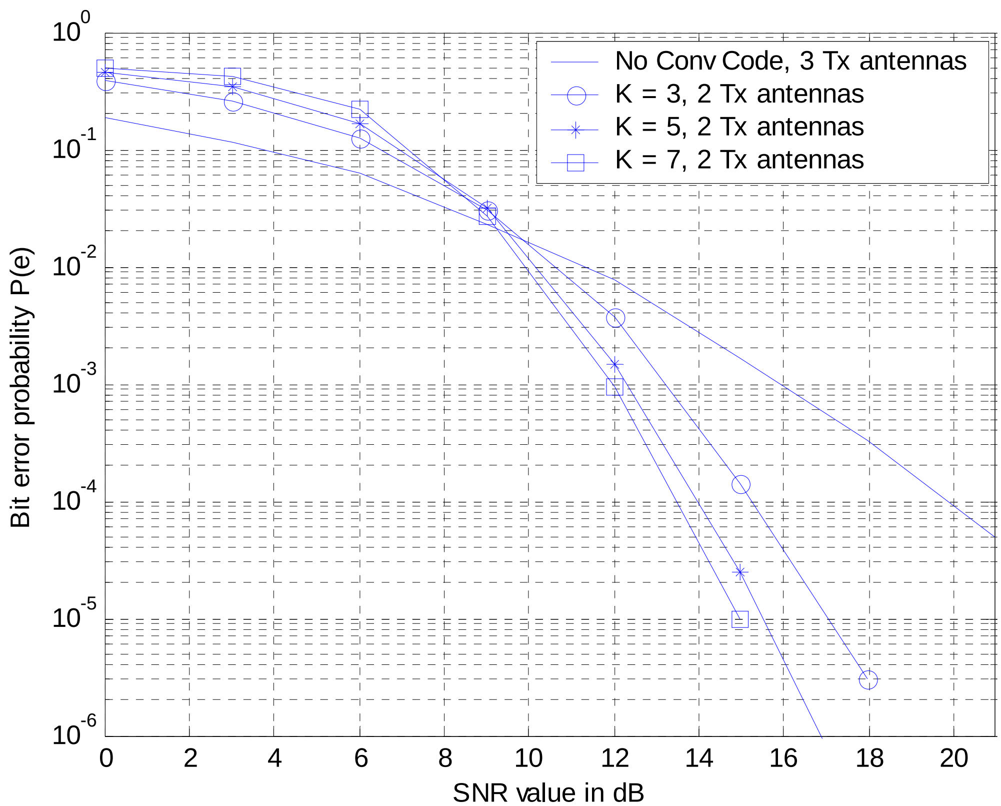


**Fig 3. 18:** Performance of 1.5 bits/s/Hz CCSBC systems

The three transmit antenna scheme employs code $G_3$ and uses 8PSK modulation. All the convolutionally concatenated systems in this simulation are two transmit antenna schemes, employ code $G_2$ and use 8PSK modulation. The convolutional codes used in this simulation are rate one-half and have constraint lengths 3, 5 and 7. These are given in table (3.1). Hard decision decoding is performed. We can see that improving the diversity by using an additional third antenna is not as advantageous as concatenation by convolutional codes for the same overall system rate.

Let us now find bounds for the performance of CCSBC systems with hard decision decoding in Rayleigh fading channels. For hard decision decoding the probability of bit error for single input convolutional coding is upper bounded by

$$P_b < \sum_{d=d_f}^{\infty} c_d D^d \Big|_{D=\sqrt{4p(1-p)}}$$

where $p$ is the probability of bit error for a binary symmetric channel. A good approximation for the probability of bit error is

$$P_b = c_{dfree} D^{dfree} \Big|_{D=\sqrt{4p(1-p)}} \tag{3.64}$$

where $d_{free}$ is the free distance of the convolutional code.

In our case of space-time coded system in a Rayleigh fading channel we may assume $p$ approximates $P_b(e)$ provided an interleaver of sufficient depth (or preferably random) is used. From (3.32)

$$p \approx P_b(e) \le \frac{1}{b'} \frac{A 2^{\frac{2N_T-1}{2}} \boldsymbol{\Gamma}\left(\frac{2N_T-1}{2}\right)}{\sqrt{2\pi E}(1+E)^{\frac{2N_T-1}{2}} (N_T-1)!}$$

$$= \rho_{N_T} \frac{1}{\sqrt{E}(1+E)^{\frac{2N_T-1}{2}}} \tag{3.65}$$

where $\rho_{N_t} = \frac{1}{b} \frac{A 2^{\frac{2N_T-1}{2}} \boldsymbol{\Gamma}\left(\frac{2N_T-1}{2}\right)}{\sqrt{2\pi}(N_T-1)!}$

Using (3.28) we get

$$P_b = 2^{dfree} c_{dfree} \left[ \frac{\rho_{N_T}}{\sqrt{E}(1+E)^{\frac{2N_T-1}{2}}} - \frac{\rho_{N_T}^2}{E(1+E)^{2N_T-1}} \right]^{\frac{dfree}{2}} \tag{3.66}$$

At large values of *SNR*,

$$P_b = 2^{dfree} c_{dfree} \rho_{N_T}^{\frac{dfree}{2}} \frac{1}{E^{\frac{N_T dfree}{2}}} \tag{3.67}$$

(3.67) shows that concatenation by convolutional codes increases the diversity order of space-time coded system by a factor of $\frac{d_{free}}{2}$ for hard decision decoding.

The error bound given by (3.66) or (3.67) is a good measure of the diversity order or slope of the *BER* curve at high *SNR*'s. It however gives a loose bound, off by more than 2 dB when compared with simulated results. The figure compares the simulation results for a 0.5 bits/s/Hz CCSBC using double output single input convolutional codes given in table (3.1) with space-time code $G_2$ and BPSK modulation.

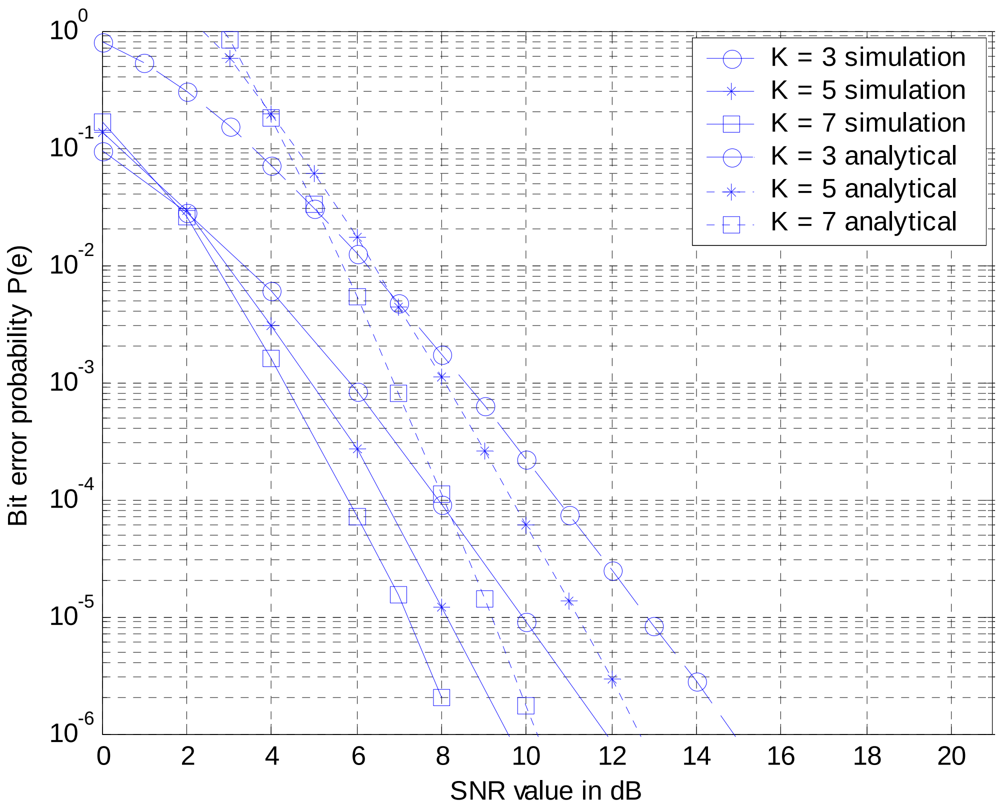


**Fig 3. 19:** Loose error bounds for CCSBC systems

A tighter bound may be obtained by evaluating the exact expression for the pair-wise error probability $P_2(d)$ given by (3.34) and (3.35) with $p$ given by (3.65). The bound for the bit error probability is then given by

$$P_b < \sum_{d=dfree}^{\infty} c_d P_2(d) \tag{3.68}$$

The figures below compare the simulation results with new tighter bound.

*Half bit per sec per Hz, CCSBC*

Figure (3.16) compares the simulated results with the tighter analytical bound given by (3.68) for 0.5 bit/s/Hz CCSBC.

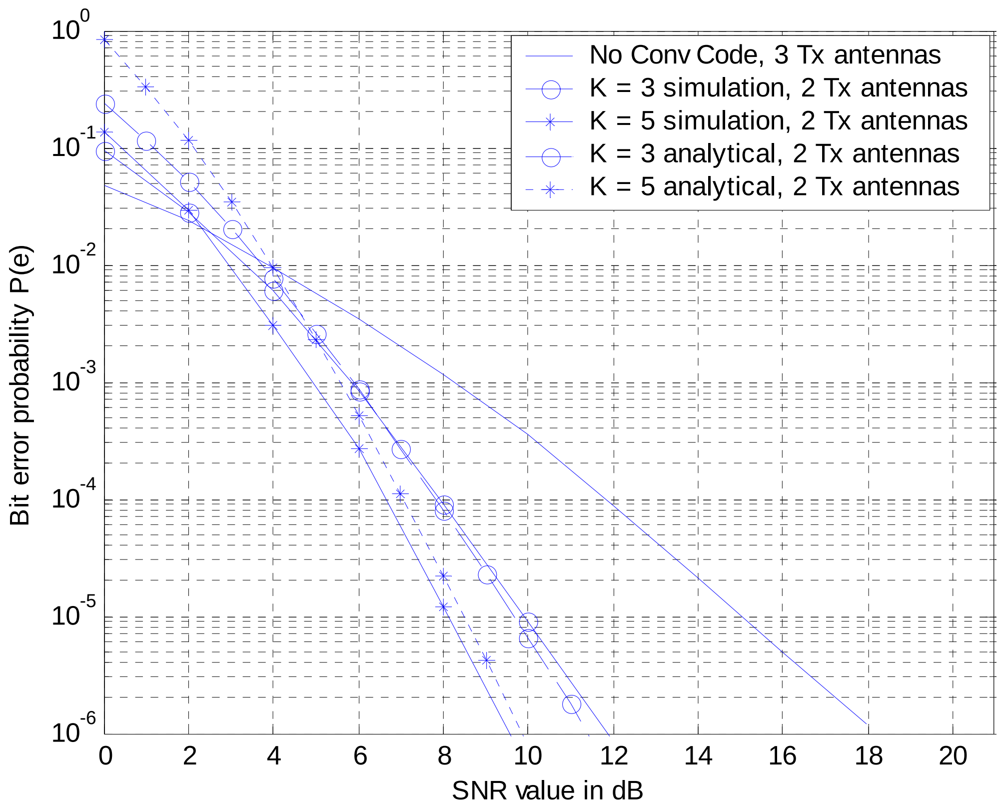


**Fig 3. 20:** Tighter bound for 0.5 bits/s/Hz CCSBC systems

*One bit per sec per Hz, CCSBC*

Figure (3.17) compares the simulated results with the tighter analytical bound given by (3.68) for 1 bit/s/Hz CCSBC.

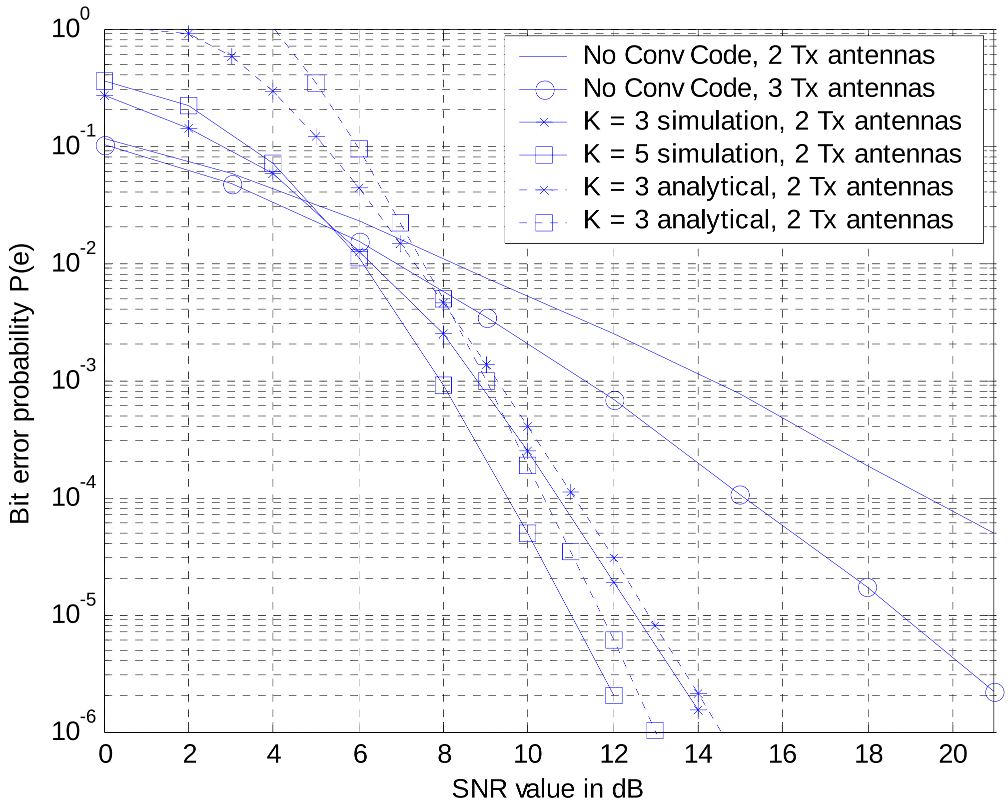


**Fig 3. 21:** Tighter bound for 1 bit/s/Hz CCSBC systems

*One and a half bit per sec per Hz, CCSBC*

Figure (3.18) compares the simulated results with the tighter analytical bound given by (3.68) for 1.5 bit/s/Hz CCSBC.

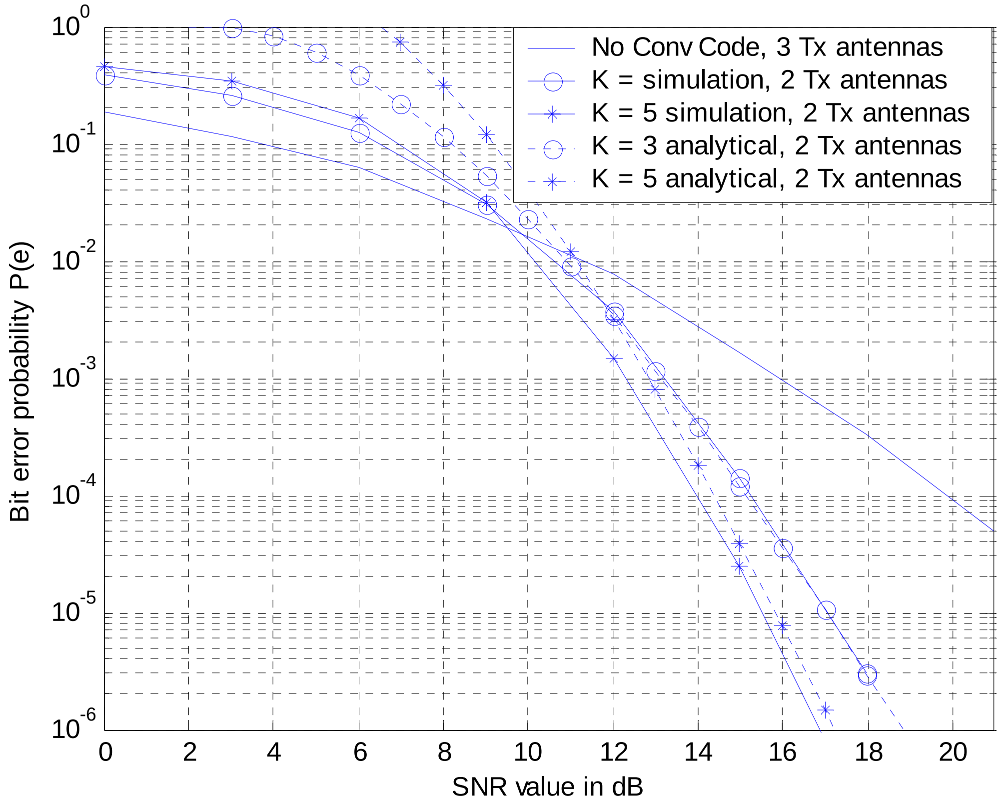


**Fig 3. 22:** Tighter bound for 1.5 bits/s/Hz CCSBC systems

***Performance of CCSBC systems with soft decision decoding***

We now consider the performance of CCSBC systems using soft decision Viterbi decoding. BPSK modulation and perfect interleaving is assumed. Bits are assumed to be transmitted at unit energy. The pair-wise error probability between the all zero path and a path at a distance $d$ from it for convolutional codes using soft Viterbi decoding is given by [13]

$$P_2(d) = P\left(\sum_{l=1}^{d} r_l' \geq 0\right) \tag{3.69}$$

where the summation represents the sum of all the bits input to the Viterbi decoder which cause the two paths to differ. Let

$$r = \sum_{l=1}^{d} r_l'$$

Using (3.11), for unit energy signaling

$$\boldsymbol{r} = \frac{1}{b}\sum_{i=1}^{N_T \times d} |\, \boldsymbol{\alpha}_i \,|^2 + \boldsymbol{\Theta}$$

where $b = rate$ of codes $G_2$, $G_3$, $G_4$ and *1* for $G_3^{'}$, $G_4^{'}$. Let $\Omega = \sum_{i=1}^{N_T \times d} |\, \boldsymbol{\alpha}_i \,|^2 = \sum_{i=1}^{N_T \times d} \alpha_i^2$ where $\boldsymbol{\alpha}_i = \alpha_i \exp(\phi)$. $\boldsymbol{\Theta}$ represents Gaussian noise with variance per complex dimension given by

$$\sigma_{\Theta x}^2 = \sigma_{\Theta y}^2 = K \frac{N_T \sum_{i=1}^{N_T \times d} |\, \boldsymbol{\alpha}_i \,|^2}{SNR} \tag{3.70}$$

where $K = \dfrac{1}{2 \times rate}$ for codes $G_2$, $G_3$, $G_4$ and *1* for $G_3^{'}$, $G_4^{'}$.

The probability $r \geq 0$ for known $\Omega$ is given by (3.12), which in our case reduces to

$$\begin{aligned} P(r \geq 0/\Omega) &= Q\left(\sqrt{\frac{\Omega SNR}{b^2 K N_T}}\right) \\ &= Q\left(\sqrt{\Omega E}\right) \end{aligned} \tag{3.71}$$

where $E = \dfrac{SNR}{b^2 K N_T}$.

The total probability is given by

$$P(r \geq 0) = \int_0^\infty P(r \geq 0/\Omega) f_\Omega(\Omega) d\Omega \tag{3.72}$$

Using (3.71) and (3.23) in (3.72) and proceeding along the same lines as in section 3.2, the total probability is calculated as

$$P(r \geq 0) = P_2(d) = \frac{2^{\frac{2N_T \times d - 1}{2}} \boldsymbol{\Gamma}\left(\frac{2N_T \times d - 1}{2}\right)}{\sqrt{2\pi E}(1+E)^{\frac{2N_T \times d - 1}{2}} (N_T \times d - 1)!} \tag{3.73}$$

For high SNRs, (3.73) shows that the diversity gain for soft decision decoding compared to hard decision decoding increases from $N_T \times d/2$ to $N_T \times d$.

The figure compares the performance of hard and soft CCSBCs that use a 2 transmit 1 receive antenna scheme. The space-time code used is $G_2$ and the modulation is BPSK. Comparisons are done for constraint lengths 3 and 5.

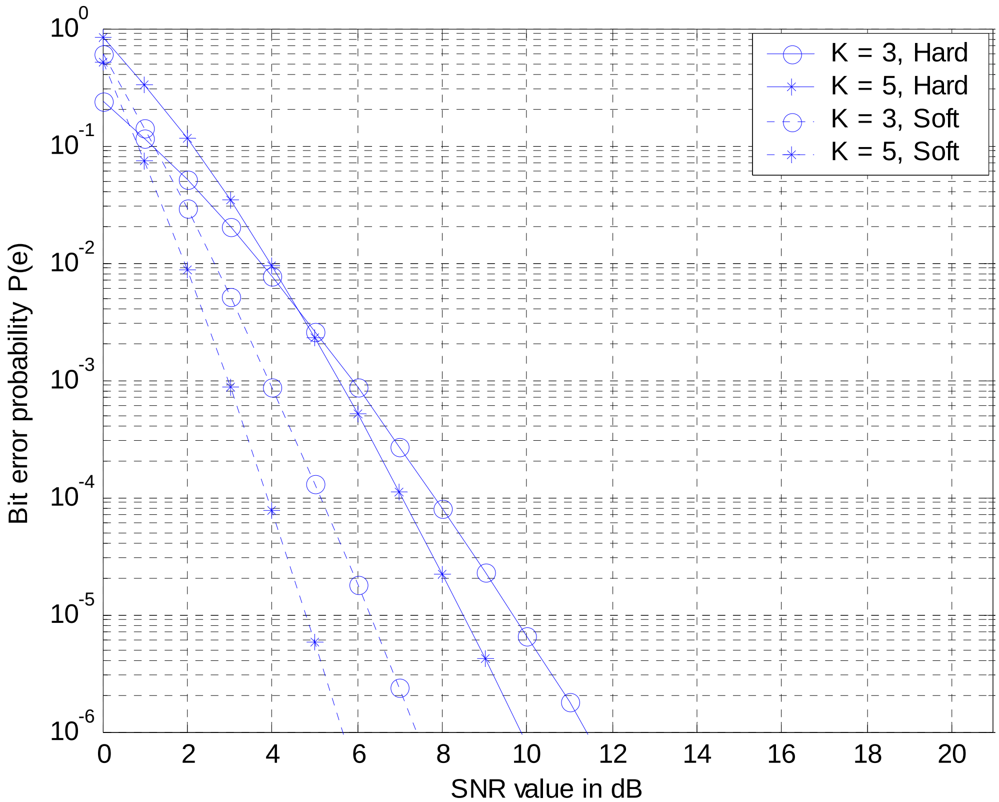


**Fig 3. 23:** 0.5 bits/s/Hz CCSBC systems with soft Viterbi decoding

The performance curves for soft decision CCSBC have a better slope than hard decision CCSBC showing that there are higher diversity gains for soft decisions.

## *3.4 Summary*

An analytic bound for the error performance of arbitrary orthogonal space-time block codes in Rayleigh fading channels was derived at the beginning of this chapter. This expression showed that introduction of space-time block codes into communication systems increased its diversity by $N_T \times N_R$. A brief introduction to convolutional codes was also given in this chapter. Expressions for the performance of convolutionally coded systems in Rayleigh fading were derived. This chapter introduced convolutionally concatenated space-time block coding schemes. General analytic expressions for the error performance of the concatenated scheme using hard and soft decision decoding were derived. These expressions showed that the diversity advantage of the concatenated scheme over ordinary communication systems was $N_T \times N_R \times dfree/2$ for hard decision decoding and $N_T \times N_R \times dfree$ for soft decision decoding. Simulation results were provided to verify the analytical results.

# Chapter 4

# Conclusions

## 4.1 Introduction

This chapter presents a brief outline of the work presented in this thesis and an outline of future work on this topic.

## 4.2 Summary of work presented in the thesis

The main emphasis of this thesis is to study the performance of space-time codes in fast fading channels and introduce serially concatenated convolutional coding as a means of improving performance. A brief outline of the original work presented in the thesis is summarized below.

1. Simulation results are provided that show how the performance of a space-time coded system is affected if the quasi-static assumption is removed. Complexity versus performance tradeoff issues are addressed for fast fading channels.
2. A general expression for the probability of error for space-time block codes in independent Rayleigh fading is derived. A similar approach has also been presented by R. Gozali et al. in [17], however a closed form generalized expression valid for any space-time block code has not been obtained. The final expression is very useful for a systems engineer to estimate the error performance for any combination of modulation scheme and space-time block code.
3. As a means of improving the error performance of a space-time block coded system, concatenation by convolutional codes is introduced in the thesis. Mathematical analysis is done and general expressions for the error performance of a convolutionally concatenated space-time block coded system in independent Rayleigh fading is derived for both hard and soft decision decoding. Simulation

results are also provided for comparison purposes. Improvement in diversity order by serial concatenation with convolutional codes is discussed. These results are important because they provide a fast way of estimating the improvement in performance by the introduction of convolutional codes without running tedious and time-consuming simulations.

## *4.3 Future work*

The improvement in performance of the concatenated scheme introduced in this work depends on the depth and type of the interleaver used. An investigation may be done to show how the performance is affected with the use of a lower interleaving depth so as to support real time voice data sensitive to interleaving delays.

To further improve the performance of space-time block coded systems, turbo-decoding methods involving an inner space-time block code and an outer convolutional code may also be investigated.

Recently diagonal algebraic space-time block codes (DAST) have been introduced by Damen M. O et al. in [18]. These are moderate complexity codes achieving full diversity at a normalized rate of 1 symbol/sec for real as well as complex constellations. An investigation on how the DAST codes behave when concatenated serially may also provide useful results for the wireless industry.

# References


[1] G. J. Foschini, Jr. and M. J. Gans, "On limits of wireless communication in a fading environment when using multiple antennas," *Wireless Personel Communications,* vol. 6, pp. 311-335, 1998.

[2] A. Narula, M. Trott, and G. Wornell, "Information theoretic analysis of multiple-antenna transmission diversity," Proc. Int. Symp. Inform. Th. Appl., Canada, Sept. 1996.

[3] E. Telatar, "Capacity of multiple-antenna Gaussian channels," AT&T-Bell Labs Internal Tech. Memo., June 1995.

[4] G. J. Foschini, Jr., "Layered space-time architecture for wireless communication in fading environment when using multi-element antennas," *Bell Labs Tech. J., pp 41-59, Autumn 1996.*

[5] N. Seshadri and J. H. Winters, "Two signaling schemes for improving the error performance of frequency-division-duplex (FDD) transmission systems using transmitter antenna diversity," *Int. J. Wireless Inform. Networks,* vol. 1, no. 1, 1994.

[6] A. Wittneben, "Base station modulation diversity for digital SIMULCAST," in *Proc. IEEE VTC,* May 1993, pp. 505-511.

[7] V. Tarokh, N. Seshadri, and A. R. Calderbank, "Space-time codes for high data rate wireless communication: Performance analysis and code construction," *IEEE Trans. Inform. Theory,* vol. 44, no. 2, pp. 744-765, Mar. 1998.

[8] S. M. Alamouti, "A simple transmitter diversity scheme for wireless communications," *IEEE J. Select. Areas Commun.,* vol. 16, pp. 1451-1458, Oct. 1998.

[9] V. Tarokh, H. Jafarkhani, and A. R. Claderbank, "Space-time block codes from orthogonal designs," *IEEE Trans. Inform. Theory.,* vol. 45, no. 5, July 1999.

[10] V. Tarokh, H. Jafarkhani, and A. R. Claderbank, "Space-time block coding for wireless communications: Performance results," *IEEE J. Select. Areas Commun.,* vol. 17, no. 3, March 1999.

[11] T.S. Rappaport, *Wireless Communications - Principles and Practice*. Prentice Hall PTR, 1996.

[12] A. Papoulis, *Probability, Random Variables, and Stochastic Processes.* McGraw-Hill, 1991.

[13] J. G. Proakis, *Digital Communications.* McGraw-Hill, 2001.

[14] L. W. Couch II, *Digital and Analog Communication Systems.* Pearson Education Asia, 2001.

[15] A. J. Viterbi, "Convolutional codes and their performance in communication systems," *IEEE Trans. Commun. Tech.,* vol. COM-19, pp. 751-772, Oct 1971.

[16] P. Frenger, P. Orten, and T. Ottosson, "Convolutional codes with optimum distance spectrum," *IEEE Commun. Lett.*, vol. 3, pp. 317-319, Nov. 1999

[17] R. Gozali, "Space-time codes for high data rate wireless communications," Ph.D thesis, Virginia Tech, 2002

[18] M. A. Damen, K. A. Meraim, and J. C. Belfiore,, "Diagonal Algebraic space-time block codes," *IEEE Trans. Inform. Theory.,* vol. 48, no. 3, March 2002.

# Vita

Saajed Ali was born in Srinagar, Kashmir, India. He received his Bachelor's degree in Electronics and Communication Engineering from Regional Engineering College, Srinagar, India in June 2001.

In the fall of 2001, he joined the Bradley Department of Electrical Engineering at Virginia Polytechnic Institute and State University, Blacksburg, Virginia as a Masters student. He has been working with Dr. Brian D. Woerner at the Mobile and Portable Radio Research Group (MPRG) since the summer of 2002. Some of the projects that he has worked on at MPRG include the implementation and analysis of wireless local area networks for high-mobility telematics sponsored by Virginia Tech Transportation Institute (VTTI) and the development of an outdoor statistical channel modeling software for ITT industries. From May 2003 he has been with Cingular Wireless as a Co-op RF engineer. At Cingular he is working on cell-site design, network performance and network optimization. He was also a member of Cingular's GSM launch team where he participated in Cingular's GSM overlay project for the Washington-Baltimore market. His research interests include channel coding, modulation, diversity techniques, channel modeling and spread-spectrum communications. Saajed Ali is also a continuing member of IEEE Inc., USA.